vectors pCR (Invitrogen), pCGN and pCAG-puro for expression in eukaryotic cells. FLAG-tagged *Trim6* cDNAs were also subcloned into pBGK1 for expression in yeast. FLAG-tagged *Myc* cDNA and cDNAs of the FLAG-tagged Myc mutants T58A, S62A and T58A/S62A, which were subcloned into the pCI vector for expression in eukaryotic cells, have been described previously (Yada et al., 2004), as has His_6-tagged ubiquitin (Okumura et al., 2004). p4×E-SVP-Luc was kindly provided by Hiroyoshi Ariga (Hokkaido University).

Recombinant proteins and antibodies

GST-fused TRIM6 was expressed in XL-1 Blue cells and then purified using glutathione-sepharose beads (GE Healthcare Bioscience, Piscataway, NJ). The recombinant TRIM6 protein was used as an immunogen in rabbits. A rabbit polyclonal anti-TRIM6 antibody was affinity purified using a recombinant TRIM6-conjugated sepharose 4B column. Other antibodies used in this study were as follows: anti-FLAG (1 μg/ml; M2 or M5, Sigma), anti-HA (1 μg/ml; HA.11, Covance Research Products, Berkeley, CA), anti-HA (1 μg/ml; Y11, Santa Cruz Biotechnology, Santa Cruz, CA), anti-His_6 (0.2 μg/ml; H-15, Santa Cruz Biotechnology), anti-Hsp90 (1 μg/ml; 68, BD, Franklin Lakes, NJ), anti-β-actin (0.2 μg/ml; AC15, Sigma), anti-Myc (1 μg/ml; N262, Santa Cruz Biotechnology and 1 μg/ml; 9E10, Covance Research Products), anti-GATA-4 (1 μg/ml; 6H10, Novus Biologicals, Littleton, CO), anti-HAND1 (1 mg/ml; GeneTex, Taiwan), anti-AFP (1:1000 dilution, 3H8, Cell Signaling Technology, Danvers, MA), anti-MAP2 (1:1000 dilution, #4542, Cell Signaling Technology), anti-Pou5f1 (Oct3/4) (1 μg/ml; mouse monoclonal, Abnova, Taiwan), and anti-Nanog (0.1 μg/ml; Abcam, Cambridge, MA).

Transfection, immunoprecipitation, and immunoblot analysis

HEK293T cells were transfected by the calcium phosphate method and lysed in a solution containing 50 mM Tris-HCl (pH 7.4), 150 mM NaCl, 1% Nonidet P-40, leupeptin (10 μg/ml), 1 mM phenylmethylsulfonyl fluoride, 400 μM Na_3VO_4, 400 μM EDTA, 10 mM NaF and 10 mM sodium pyrophosphate. The cell lysates were centrifuged at 16,000 ***g*** for 15 minutes at 4℃, and the resulting supernatant was incubated with antibodies for 2 hours at 4℃. Protein A-sepharose (GE Healthcare) that had been equilibrated with the same solution was added to the mixture, which was then tumbled for 1 hour at 4℃. The resin was separated by centrifugation, washed five times with ice-cold lysis buffer and then boiled in SDS sample buffer. Immune complexes were detected with primary antibodies, horseradish peroxidase-conjugated antibodies to mouse or rabbit IgG (1:10,000 dilutions, Promega) and an enhanced chemiluminescence system (GE Healthcare). For small-scale transfection, Fugene HD reagent (Roche, Mannheim, Germany) was used according to the manufacturer's protocol.

Ni-NTA pull-down assay

Cell lysates containing 8 M urea were used for purification of His_6-ubiquitin-conjugated proteins by chromatography on ProBond resin (Invitrogen) and proteins were then eluted from the resin with a solution containing 50 mM sodium phosphate buffer (pH 8.0), 100 mM KCl, 20% glycerol, 0.2% NP-40 and 200 mM imidazole (Okumura et al., 2004).

Establishment of stable transfectants by using a retrovirus expression system

Complementary DNAs were subcloned into pMX-puro or pMX-neo (kindly provided by Toshio Kitamura, Tokyo University). The resulting vectors were used to transfect Plat A or Plat E cells, and recombinant retroviruses were then generated (Morita et al., 2000). Forty-eight hours after transfection, culture supernatants were harvested and used for infection. The infection was carried out in the presence of polybrene at 8 μg/ml (Sigma-Aldrich). The infected clones were expanded and selected in a medium containing puromycin (1 μg/ml for E14 and NIH 3T3 and 5 μg/ml for Namalwa, Sigma-Aldrich) and G418 (250 μg/ml for E14, Sigma-Aldrich).

Establishment of stable transfectants of ES cells by using electroporation

E14 cells (2.5×10^7 cells) were electroporated with linearized pCAG-puro-FLAG-TRIM6 plasmid (20 μg) at 300 V and 125 μF twice by using Gene Pulser X cell (Bio-Rad Laboratories, Hercules, CA). The cells were plated onto 60-mm dishes and puromycin selection (1 μg/ml; Sigma-Aldrich) was initiated from 2 days after electroporation. After selection on a medium containing puromycin, the resulting cell lines were checked by immunoblot analysis with an anti-FLAG antibody.

RNA interference

pSUPER-retro-puro vector was purchased from OligoEngine. An shRNA for mouse TRIM6 mRNA was designed according to a previous report (Elbashir et al., 2002) and chemically synthesized (Invitrogen). pSUPER-retro-puro containing an shRNA for the mouse TRIM6 sequence (sh-TRIM6-1, 5′-GAGGCTCAG-AGAGGTTGCG-3′ or sh-TRIM6-2, 5′-GGGGCTGAGCATCATAGAA-3′) was constructed according to the manufacturer's protocol. We also used a scrambled shRNA as a negative control with no significant homology to any known gene sequences in the human or mouse genomes. Approximately 50% confluent HEK293 cells in 100-mm dishes were transfected with 10 μg pSUPER-retro-puro-shTRIM6 or scrambled shRNA vector together with 10 μg amphotrophic-packaging plasmid pCL10A1 using Fugene HD reagent (Roche). Forty-eight hours after transfection, culture supernatant containing retrovirus was collected, and retroviral supernatant was added to ES cells in 60-mm dishes with polybrene (8 μg/ml, Sigma-Aldrich). Cells were cultured with puromycin (1 μg/ml) and LIF for 1 week.

Dual-luciferase assay

Cells were seeded in 24-well plates at 1×10^5 cells or 5×10^4 cells per well for HEK293T or E14, respectively, and incubated at 37℃ with 5% CO_2 for 48 hours. A p4×E-SVP-Luc reporter plasmid, pRL-TK *Renilla* luciferase plasmid (Promega) and various combinations of HA-tagged TRIM6 and/or FLAG-tagged Myc expression plasmid were transfected into cells using Fugene HD reagent (Roche). Forty-eight hours after transfection, the cell lysates were assayed for luciferase activity with a Dual-Luciferase Reporter Assay System (Promega) and quantified with a luminometer (Promega).

Protein stability assay with cycloheximide

Cells were cultured with cycloheximide (Sigma-Aldrich) at a concentration of 50 μg/ml and then incubated for the indicated times in each experiment.

Immunofluorescence staining

E14 cells expressing FLAG-tagged TRIM6 grown on a glass cover were fixed for 10 minutes at room temperature with 2% formaldehyde in PBS and then incubated for 1 hour at room temperature with a primary antibody to FLAG or Myc in PBS containing 0.1% bovine serum albumin and 0.1% saponin. The cells were then incubated with Alexa-Fluor-488-labeled goat polyclonal antibody to mouse IgG or Alexa-Fluor-546-labeled goat polyclonal antibody to rabbit IgG (Invitrogen) at a dilution of 1:1000. The cells were further incubated with Hoechst 33258 (1 μg/ml) in PBS for 10 minutes, followed by extensive washing with PBS, and then photographed with a CCD camera (DP71, Olympus) attached to an Olympus BX51 microscope.

Real-time PCR

Total RNA was isolated from E14 cells using ISOGEN (Nippon Gene, Tokyo, Japan), followed by reverse transcription (RT) by ReverTra Ace (Toyobo, Osaka, Japan). The resulting cDNA was subjected to real-time PCR with a StepOne machine and Power SYBR Green PCR master mix (Applied Biosystems, Foster City, CA). The average threshold cycle (Ct) was determined from independent experiments and the level of gene expression relative to *GAPDH* was determined. The primer sequences for *Trim6*, *Ccnd1* and *Gapdh* were as follows: *Trim6*, 5′-CGATCTCAGGAGCACCGTGGT-3′ and 5′-AGGATGCTTCGGAGCTGCTTA-3′; *Ccnd1*, 5′-CCTCTCCTGCTACCGCACAAC-3′ and 5′-GCGCAGGCTTG-ACTCCAGAAG-3′; and *Gapdh*, 5′-GCAAATTCCATGGCACCGT-3′ and 5′-TCGCCCCACTTGATTTTGG-3′.

ES cells in ground state culture

As previously described (Ying et al., 2008), pre-formulated NDiff N2B27 base medium (StemCells, Inc., Newark, CA) was prepared with CHIR99021 (Axon Medchem BV, Groningen, Netherlands) and PD0325901 (Sigma-Aldrich). Inhibitors were used at the following concentrations: CHIR99021, 3 μM; and PD0325901, 1 μM (2i). ES cells were routinely propagated by trypsinization and replating every 3 days, with a ratio of 1:10.

Statistical analysis

Student's *t*-test was used to determine the statistical significance of experimental data.

Acknowledgements

We would like to thank Toshio Kitamura (Tokyo University) and Hiroyoshi Ariga (Hokkaido University) for the plasmids and Yuri Soida for help in preparing the manuscript.

Funding

The work was supported, in part, by Grants-in-Aid for Scientific Research from the Ministry of Education, Culture, Sports, Science and Technology (18076001 and 21390087), Grant for Basic Science Research Projects from The Sumitomo Foundation, The Suhara Foundation and The Kudo Science Foundation.

References

Aravind, L. and Koonin, E. V. (2000). The U box is a modified RING finger - a common domain in ubiquitination. *Curr. Biol.* **10**, R132-R134.

Bahram, F., von der Lehr, N., Cetinkaya, C. and Larsson, L. G. (2000). Myc hot spot mutations in lymphomas result in inefficient ubiquitination and decreased proteasome-mediated turnover. *Blood* **95**, 2104-2110.

Cartwright, P., McLean, C., Sheppard, A., Rivett, D., Jones, K. and Dalton, S. (2005). LIF/STAT3 controls ES cell self-renewal and pluripotency by a Myc-dependent mechanism. *Development* **132**, 885-896.

Chan, K. K., Zhang, J., Chia, N. Y., Chan, Y. S., Sim, H. S., Tan, K. S., Oh, S. K., Ng, H. H. and Choo, A. B. (2009). KLF4 and PBX1 directly regulate NANOG expression in human embryonic stem cells. *Stem Cells* **27**, 2114-2125.

Cyr, D. M., Hohfeld, J. and Patterson, C. (2002). Protein quality control: U-box-containing E3 ubiquitin ligases join the fold. *Trends Biochem. Sci.* **27**, 368-375.

Daksis, J. I., Lu, R. Y., Facchini, L. M., Marhin, W. W. and Penn, L. J. (1994). Myc induces cyclin D1 expression in the absence of de novo protein synthesis and links mitogen-stimulated signal transduction to the cell cycle. *Oncogene* **9**, 3635-3645.

Dang, C. V. (1999). Myc target genes involved in cell growth, apoptosis, and metabolism. *Mol. Cell. Biol.* **19**, 1-11.

Darr, H., Mayshar, Y. and Benvenisty, N. (2006). Overexpression of NANOG in human ES cells enables feeder-free growth while inducing primitive ectoderm features. *Development* **133**, 1193-1201.

Elbashir, S. M., Harborth, J., Weber, K. and Tuschl, T. (2002). Analysis of gene function in somatic mammalian cells using small interfering RNAs. *Methods* **26**, 199-213.

Freemont, P. S. (2000). RING for destruction? *Curr. Biol.* **10**, R84-R87.

Hatakeyama, S., Yada, M., Matsumoto, M., Ishida, N. and Nakayama, K. I. (2001). U box proteins as a new family of ubiquitin-protein ligases. *J. Biol. Chem.* **276**, 33111-33120.

Hershko, A. and Ciechanover, A. (1992). The ubiquitin system for protein degradation. *Annu. Rev. Biochem.* **61**, 761-807.

Hershko, A. and Ciechanover, A. (1998). The ubiquitin system. *Annu. Rev. Biochem.* **67**, 425-479.

Hershko, A., Heller, H., Elias, S. and Ciechanover, A. (1983). Components of ubiquitin-protein ligase system. Resolution, affinity purification, and role in protein breakdown. *J. Biol. Chem.* **258**, 8206-8214.

Hishida, T., Nozaki, Y., Nakachi, Y., Mizuno, Y., Okazaki, Y., Ema, M., Takahashi, S., Nishimoto, M. and Okuda, A. (2011). Indefinite self-renewal of ESCs through Myc/Max transcriptional complex-independent mechanisms. *Cell Stem Cell* **9**, 37-49.

Huibregtse, J. M., Scheffner, M., Beaudenon, S. and Howley, P. M. (1995). A family of proteins structurally and functionally related to the E6-AP ubiquitin-protein ligase. *Proc. Natl. Acad. Sci. USA* **92**, 2563-2567.

Joazeiro, C. A. and Weissman, A. M. (2000). RING finger proteins: mediators of ubiquitin ligase activity. *Cell* **102**, 549-552.

Kano, S., Miyajima, N., Fukuda, S. and Hatakeyama, S. (2008). Tripartite motif protein 32 facilitates cell growth and migration via degradation of Abl-interactor 2. *Cancer Res.* **68**, 5572-5580.

Kim, S. Y., Herbst, A., Tworkowski, K. A., Salghetti, S. E. and Tansey, W. P. (2003). Skp2 regulates Myc protein stability and activity. *Mol. Cell* **11**, 1177-1188.

Knoepfler, P. S., Cheng, P. F. and Eisenman, R. N. (2002). N-Myc is essential during neurogenesis for the rapid expansion of progenitor cell populations and the inhibition of neuronal differentiation. *Genes Dev.* **16**, 2699-2712.

Knofler, M., Meinhardt, G., Bauer, S., Loregger, T., Vasicek, R., Bloor, D. J., Kimber, S. J. and Husslein, P. (2002). Human Hand1 basic helix-loop-helix (bHLH) protein: extra-embryonic expression pattern, interaction partners and identification of its transcriptional repressor domains. *Biochem. J.* **361**, 641-651.

Kunath, T., Saba-El-Leil, M. K., Almousailleakh, M., Wray, J., Meloche, S. and Smith, A. (2007). FGF stimulation of the Erk1/2 signalling cascade triggers transition of pluripotent embryonic stem cells from self-renewal to lineage commitment. *Development* **134**, 2895-2902.

Kwon, G. S., Fraser, S. T., Eakin, G. S., Mangano, M., Isern, J., Sahr, K. E., Hadjantonakis, A. K. and Baron, M. H. (2006). TAfp-GFP) expression marks primitive and definitive endoderm lineages during mouse development. *Dev. Dyn.* **235**, 2549-2558.

Lorick, K. L., Jensen, J. P., Fang, S., Ong, A. M., Hatakeyama, S. and Weissman, A. M. (1999). RING fingers mediate ubiquitin-conjugating enzyme (E2)-dependent ubiquitination. *Proc. Natl. Acad. Sci. USA* **96**, 11364-11369.

Lutterbach, B. and Hann, S. R. (1994). Hierarchical phosphorylation at N-terminal transformation-sensitive sites in Myc protein is regulated by mitogens and in mitosis. *Mol. Cell. Biol.* **14**, 5510-5522.

Meroni, G. and Diez-Roux, G. (2005). TRIM/RBCC, a novel class of 'single protein RING finger' E3 ubiquitin ligases. *BioEssays* **27**, 1147-1157.

Miyajima, N., Maruyama, S., Bohgaki, M., Kano, S., Shigemura, M., Shinohara, N., Nonomura, K. and Hatakeyama, S. (2008). TRIM68 regulates ligand-dependent transcription of androgen receptor in prostate cancer cells. *Cancer Res.* **68**, 3486-3494.

Morita, S., Kojima, T. and Kitamura, T. (2000). Plat-E: an efficient and stable system for transient packaging of retroviruses. *Gene Ther.* **7**, 1063-1066.

Nakagawa, M., Koyanagi, M., Tanabe, K., Takahashi, K., Ichisaka, T., Aoi, T., Okita, K., Mochiduki, Y., Takizawa, N. and Yamanaka, S. (2008). Generation of induced pluripotent stem cells without Myc from mouse and human fibroblasts. *Nat. Biotechnol.* **26**, 101-106.

Nisole, S., Stoye, J. P. and Saib, A. (2005). TRIM family proteins: retroviral restriction and antiviral defence. *Nat. Rev. Microbiol.* **3**, 799-808.

Niwa, H., Burdon, T., Chambers, I. and Smith, A. (1998). Self-renewal of pluripotent embryonic stem cells is mediated via activation of STAT3. *Genes Dev.* **12**, 2048-2060.

Niwa, H., Miyazaki, J. and Smith, A. G. (2000). Quantitative expression of Oct-3/4 defines differentiation, dedifferentiation or self-renewal of ES cells. *Nat. Genet.* **24**, 372-376.

Niwa, H., Ogawa, K., Shimosato, D. and Adachi, K. (2009). A parallel circuit of LIF signalling pathways maintains pluripotency of mouse ES cells. *Nature* **460**, 118-122.

Okita, K., Nakagawa, M., Hyenjong, H., Ichisaka, T. and Yamanaka, S. (2008). Generation of mouse induced pluripotent stem cells without viral vectors. *Science* **322**, 949-953.

Okumura, F., Hatakeyama, S., Matsumoto, M., Kamura, T. and Nakayama, K. I. (2004). Functional regulation of FEZ1 by the U-box-type ubiquitin ligase E4B contributes to neuritogenesis. *J. Biol. Chem.* **279**, 53533-53543.

Ozato, K., Shin, D. M., Chang, T. H. and Morse, H. C., 3rd. (2008). TRIM family proteins and their emerging roles in innate immunity. *Nat. Rev. Immunol* **8**, 849-860.

Perez-Roger, I., Kim, S. H., Griffiths, B., Sewing, A. and Land, H. (1999). Cyclins D1 and D2 mediate Myc-induced proliferation via sequestration of p27(Kip1) and p21(Cip1). *EMBO J.* **18**, 5310-5320.

Peters, J. M. (1998). SCF and APC: the Yin and Yang of cell cycle regulated proteolysis. *Curr. Opin. Cell Biol.* **10**, 759-768.

Quaderi, N. A., Schweiger, S., Gaudenz, K., Franco, B., Rugarli, E. I., Berger, W., Feldman, G. J., Volta, M., Andolfi, G., Gilgenkrantz, S. et al. (1997). Opitz G/BBB syndrome, a defect of midline development, is due to mutations in a new RING finger gene on Xp22. *Nat. Genet.* **17**, 285-291.

Reymond, A., Meroni, G., Fantozzi, A., Merla, G., Cairo, S., Luzi, L., Riganelli, D., Zanaria, E., Messali, S., Cainarca, S. et al. (2001). The tripartite motif family identifies cell compartments. *EMBO J.* **20**, 2140-2151.

Satoh, Y., Matsumura, I., Tanaka, H., Ezoe, S., Sugahara, H., Mizuki, M., Shibayama, H., Ishiko, E., Ishiko, J., Nakajima, K. et al. (2004). Roles for Myc in self-renewal of hematopoietic stem cells. *J. Biol. Chem.* **279**, 24986-24993.

Scheffner, M., Nuber, U. and Huibregtse, J. M. (1995). Protein ubiquitination involving an E1-E2-E3 enzyme ubiquitin thioester cascade. *Nature* **373**, 81-83.

Soudais, C., Bielinska, M., Heikinheimo, M., MacArthur, C. A., Narita, N., Saffitz, J. E., Simon, M. C., Leiden, J. M. and Wilson, D. B. (1995). Targeted mutagenesis of the transcription factor GATA-4 gene in mouse embryonic stem cells disrupts visceral endoderm differentiation in vitro. *Development* **121**, 3877-3888.

Takahashi, K. and Yamanaka, S. (2006). Induction of pluripotent stem cells from mouse embryonic and adult fibroblast cultures by defined factors. *Cell* **126**, 663-676.

Takayama, N., Nishimura, S., Nakamura, S., Shimizu, T., Ohnishi, R., Endo, H., Yamaguchi, T., Otsu, M., Nishimura, K., Nakanishi, M. et al. (2010). Transient activation of Myc expression is critical for efficient platelet generation from human induced pluripotent stem cells. *J. Exp. Med.* **207**, 2817-2830.

Tian, L., Wu, X., Lin, Y., Liu, Z., Xiong, F., Han, Z., Zhou, Y., Zeng, Q., Wang, Y., Deng, J. et al. (2009). Characterization and potential function of a novel pre-implantation embryo-specific RING finger protein: TRIML1. *Mol. Reprod Dev.* **76**, 656-664.

Tropepe, V., Hitoshi, S., Sirard, C., Mak, T. W., Rossant, J. and van der Kooy, D. (2001). Direct neural fate specification from embryonic stem cells: a primitive mammalian neural stem cell stage acquired through a default mechanism. *Neuron* **30**, 65-78.

van Riggelen, J., Yetil, A. and Felsher, D. W. (2010). MYC as a regulator of ribosome biogenesis and protein synthesis. *Nat. Rev. Cancer* **10**, 301-309.

von der Lehr, N., Johansson, S., Wu, S., Bahram, F., Castell, A., Cetinkaya, C., Hydbring, P., Weidung, I., Nakayama, K., Nakayama, K. I. et al. (2003). The F-box protein Skp2 participates in Myc proteosomal degradation and acts as a cofactor for Myc-regulated transcription. *Mol. Cell* **11**, 1189-1200.

Watanabe, S., Umehara, H., Murayama, K., Okabe, M., Kimura, T. and Nakano, T. (2006). Activation of Akt signaling is sufficient to maintain pluripotency in mouse and primate embryonic stem cells. *Oncogene* **25**, 2697-2707.

Watt, F. M., Frye, M. and Benitah, S. A. (2008). Myc in mammalian epidermis: how can an oncogene stimulate differentiation? *Nat. Rev. Cancer* **8**, 234-242.

Wilson, A., Murphy, M. J., Oskarsson, T., Kaloulis, K., Bettess, M. D., Oser, G. M., Pasche, A. C., Knabenhans, C., Macdonald, H. R. and Trumpp, A. (2004). Myc controls the balance between hematopoietic stem cell self-renewal and differentiation. *Genes Dev.* **18**, 2747-2763.

Yada, M., Hatakeyama, S., Kamura, T., Nishiyama, M., Tsunematsu, R., Imaki, H., Ishida, N., Okumura, F., Nakayama, K. and Nakayama, K. I. (2004). Phosphorylation-dependent degradation of Myc is mediated by the F-box protein Fbw7. *EMBO J.* **23**, 2116-2125.

Ying, Q. L., Wray, J., Nichols, J., Batlle-Morera, L., Doble, B., Woodgett, J., Cohen, P. and Smith, A. (2008). The ground state of embryonic stem cell self-renewal. *Nature* **453**, 519-523.

Gene 497 (2012) 110–115

Contents lists available at SciVerse ScienceDirect

Gene

journal homepage: www.elsevier.com/locate/gene

Short Communication

Somatic mosaicism in two unrelated patients with X-linked chronic granulomatous disease characterized by the presence of a small population of normal cells

Masafumi Yamada [a,*], Yuka Okura [a], Yasuto Suzuki [b], Shinobu Fukumura [c], Toru Miyazaki [d], Hisami Ikeda [d], Shun-Ichiro Takezaki [a], Nobuaki Kawamura [a], Ichiro Kobayashi [a], Tadashi Ariga [a]

[a] Department of Pediatrics, Hokkaido University Graduate School of Medicine, Sapporo, 060-8638, Japan
[b] Department of Pediatrics, Kushiro Red Cross Hospital, Kushiro, 085-8512, Japan
[c] Department of Pediatrics, Kushiro City General Hospital, Kushiro, 085-0822, Japan
[d] Hokkaido Red Cross Blood Center, Sapporo, 063-0002, Japan

ARTICLE INFO

Article history:
Accepted 17 January 2012
Available online 28 January 2012

Keywords:
X-linked chronic granulomatous disease (X-CGD)
Cytochrome b_{558} β (CYBB)
Somatic mosaicism
De novo mutation
Reversion

ABSTRACT

X-linked chronic granulomatous disease (X-CGD) is a primary immunodeficiency disease of phagocytes caused by mutations in the *cytochrome b_{558} β (CYBB)* gene. We, for the first time, detected somatic mosaicism in two unrelated male patients with X-CGD caused by *de novo* nonsense mutations (p.Gly223X and p.Glu462X) in the *CYBB* gene. In each patient, a small subset of granulocytes was normal in terms of respiratory burst (ROB) activity, $gp91^{phox}$ expression, and *CYBB* sequences. Cells with wild-type *CYBB* sequence were also detected in buccal swab specimens and in peripheral blood mononuclear cells. The normal cells were shown to be of the patient origin by fluorescent *in situ* hybridization analysis of X/Y chromosomes, and by HLA DNA typing. Two possible mechanisms for this somatic mosaicism were considered. The first is that the *de novo* disease-causing mutations in *CYBB* occurred at an early multicellular stage of embryogenesis with subsequent expansion of the mutated cells, leaving some unmutated cells surviving. The second possibility is that the *de novo* mutations occurred in oocytes which was followed by reversion of the mutations in a small subset of cells in early embryogenesis.

1. Introduction

Chronic granulomatous disease (CGD) is a primary immunodeficiency disease (PID) caused by mutations in one of five genes encoding subunits of the nicotinamide dinucleotide phosphate (NADPH) oxidase complex, leading to defective production of superoxide and other reactive oxygen species in phagocytic cells (Malech and Gallin, 1987; Matute et al., 2009). The most common form is X-linked recessive CGD (X-CGD), which results from mutations in the *cytochrome b_{558} β (CYBB)* gene encoding $gp91^{phox}$ (Winkelstein et al., 2000).

Somatic mosaicism has recently been identified in various genetic diseases. This mosaicism can be due to *de novo* mutations that occur during embryogenesis, or to reversion of inherited mutations (Hirschhorn, 2003). The former is associated with highly variable mosaicism and may be accompanied by germ line mosaicism depending on the stage of embryogenesis in which the mutation occurs (Frank, 2010; Hirschhorn, 2003). The latter has been reported in several disorders, including PIDs, in which the reversion gives a growth advantage to the corrected cells (Hirschhorn, 2003). The critical difference is that it can be shown that the mutation that reverted to normal had been inherited from a parent (Hirschhorn, 2003).

In this study, we, for the first time, have demonstrated somatic mosaicism in two unrelated male patients with X-CGD caused by *de novo* nonsense mutations in the *CYBB* gene.

2. Materials and methods

2.1. Patients

Patient 1 was a 13-year-old male born to non-consanguineous Japanese parents. At birth, he had preaxial polydactyly of the right hand. He had borderline developmental delay noticed at the age of 5 months. Recurrent perianal abscesses and lymphadenitis led to the diagnosis of X-CGD at the age of 1 year. He mistakenly received BCG vaccination at the age of 7 years without significant complications, with a prophylactic treatment with isoniazid for 6 months. He developed a liver abscess at the age of 12 years which required surgical

Abbreviations: X-CGD, X-linked chronic granulomatous disease; *CYBB, cytochrome b_{558} β*; ROB, respiratory burst; PBMC, peripheral blood mononuclear cells; PID, primary immunodeficiency disease; EBV-LCLs, EBV-transformed lymphoblastoid cell lines.

* Corresponding author at: Department of Pediatrics, Hokkaido University Graduate School of Medicine, North 15 West 7, Kita-ku Sapporo, 060-8638, Japan. Tel.: +81 11 706 5954; fax: +81 11 7067898.
E-mail address: yamadam@med.hokudai.ac.jp (M. Yamada).

0378-1119/$ – see front matter © 2012 Elsevier B.V. All rights reserved.
doi:10.1016/j.gene.2012.01.019

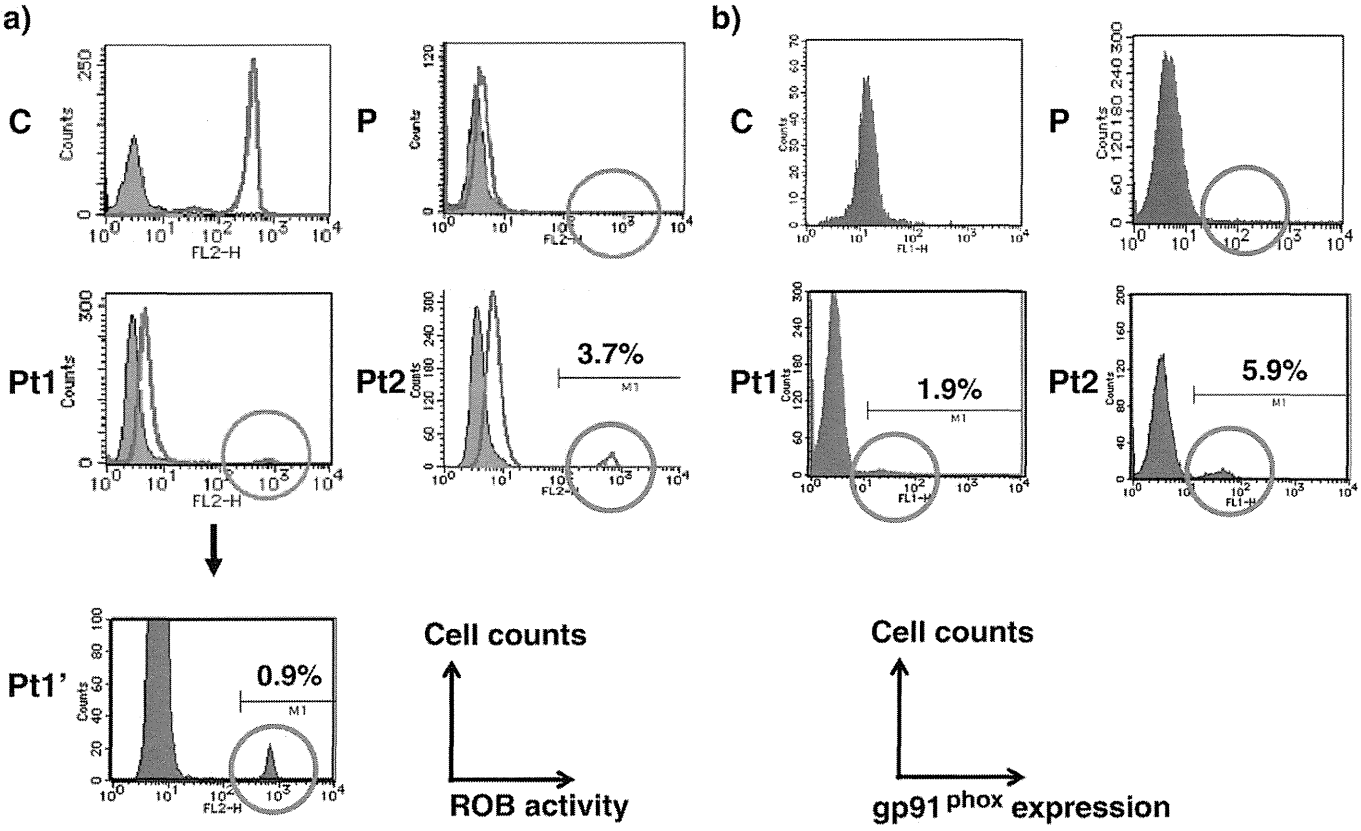

Fig.1. Respiratory burst (ROB) analysis and surface gp91^{phox} expression in granulocytes. (a) ROB analysis of granulocytes left unstimulated (filled orange) or stimulated with phorbol myristate acetate (empty blue). (b) Granulocyte surface gp91^{phox} expression. C: a normal control, P: a typical X-CGD patient, Pt1: Patient 1, Pt1': An enlarged view of Patient 1's ROB result, Pt2: Patient 2.

resection. Patient 2 was a 2-year-old male with a history of BCG lymphadenitis at the age of 1 year, which was controlled by treatment with isoniazid for 6 months. He developed persistent diarrhea with liver dysfunction at the age of 2 years, which was controlled by oral steroid treatment. Both patients have no history of transfusion.

2.2. Flow cytometric analysis of granulocyte respiratory burst (ROB) activity and surface gp91^{phox} expression

These analyses were performed following the methods described elsewhere (Yamada et al., 2000).

2.3. Enrichment of gp91^{phox} + cells

Granulocytes were first Fc-blocked with the patient's own serum to avoid possible contamination of the cells by foreign DNA from commercially obtained AB sera. The cells were reacted with monoclonal mouse anti-gp91^{phox} antibody, 7D5 provided by Dr. M. Nakamura, washed three times, then reacted with anti-mouse IgG1 conjugated with magnetic beads (Miltenyi Biotec, Auburn CA, USA). The enriched population of gp91^{phox} + cells was obtained by positive selection with MACS sorting (Miltenyi Biotec).

2.4. Studies of direct sequencing and TA clones of CYBB

Informed consent for genetic analysis was obtained from the patients, their mothers, and normal controls under a protocol approved by the Institutional Review Board (IRB) of Hokkaido University Hospital. Genomic DNA was extracted from heparinized blood or buccal swab samples using SepaGene (Sankojunyaku, Tokyo, Japan). PCR and sequencing conditions were described elsewhere (Ariga et al., 1998). PCR primers used for genomic DNA were located in the flanking regions of each exon in *CYBB* as reported (Hui et al., 1997). Nucleotide number 1 corresponds to the A of the ATG translation–initiation codon. The presence of wild-type sequences was confirmed by sequencing TA clones obtained with the TOPO-TA cloning kit (Invitrogen, Carlsbad, CA, USA) following the manufacturer's instructions.

2.5. Generation of EBV-transformed cell lines (EBV-LCLs)

EBV-LCLs were generated by *in vitro* transformation of human B cells with EBV (strain B95-8), as described elsewhere (Tosato and Cohen, 2007).

2.6. HLA DNA typing study

This study was performed following the methods described elsewhere (Ariga et al., 2001a, 2001b). Briefly, DNA typing for identification of HLA class I alleles was performed by PCR-SSOP (Sequence Specific Oligonucleotide Probe) with Luminex 100 xMAP flow cytometry dual-laser system to quantitate fluorescently labeled oligonucleotides attached to color-coded microbeads. Type of HLA class I was determined using WAKFlow HLA Typing (purchased from Wakunaga Pharmaceutical, Hiroshima, Japan).

2.7. Monocyte-derived macrophages and dendritic cells

Isolated peripheral blood mononuclear cells (PBMC) were seeded in a 6-well culture plate at a density of 5×10^6/ml. After incubation at 37 °C in a 5% CO_2 incubator for an hour, nonadherent cells were removed with vigorous pipetting with prewarmed RPMI1640 to obtain adherent monocytes. The adherent monocytes were then differentiated

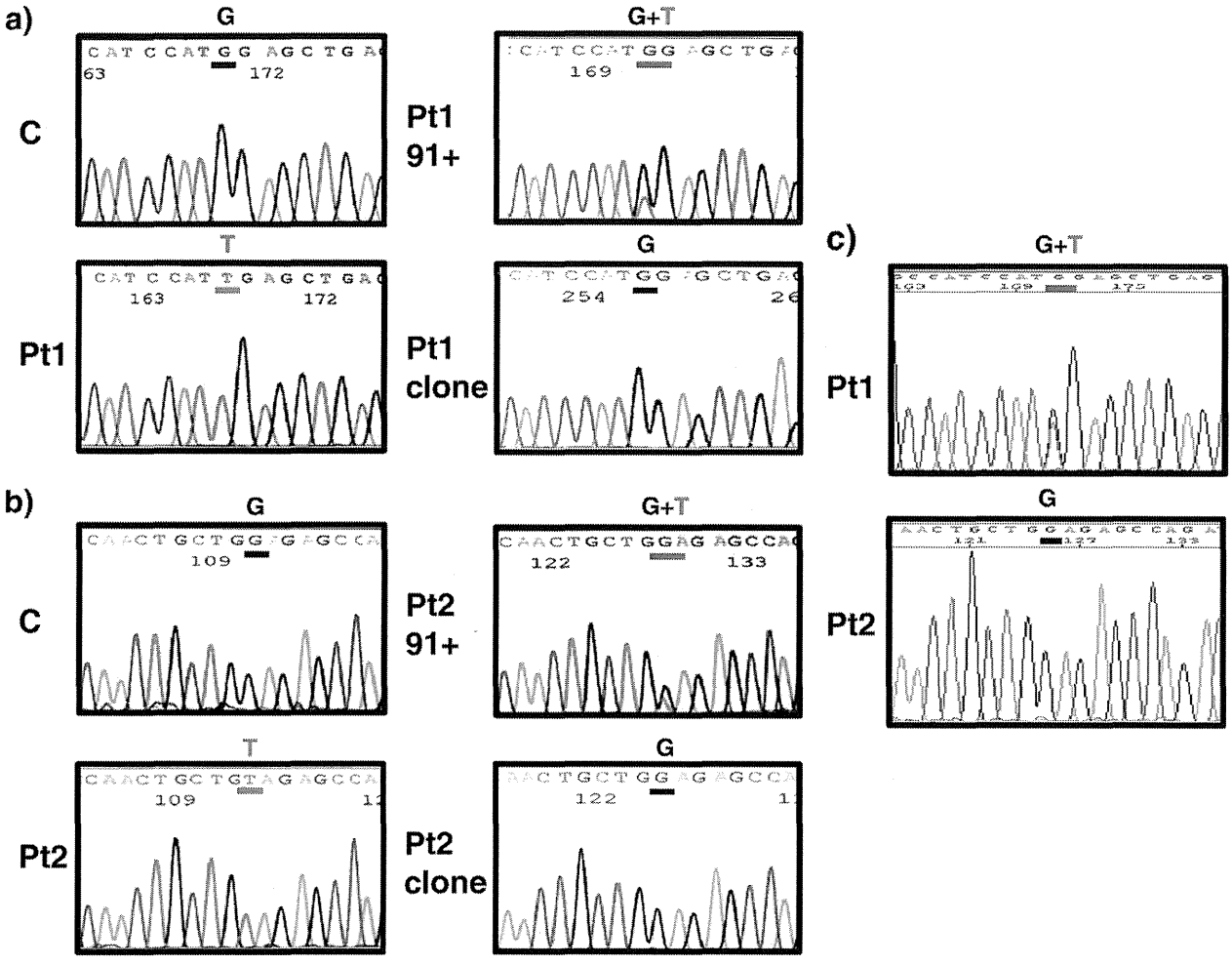

Fig. 2. Sequence analysis of the *CYBB* gene. (a) Sequence analysis of *CYBB* exon 6 in Patient 1. (b) Sequence analysis of *CYBB* exon 11 in Patient 2. (c) Sequence analysis of *CYBB* exon 6 and exon 11 in EBV-LCLs from Patient 1 (Pt1) and Patient 2 (Pt2), respectively. C: a control. Pt1: Patient 1. Pt2: Patient 2. 91+: gp91^{phox}-enriched granulocytes. Clone: a TA clone with wild-type sequence.

into macrophages by culturing for 7 days in RPMI1640 containing 10% fetal bovine serum in the presence of 5 ng/ml of GM-CSF (R&D, Minneapolis, MN) or 10 ng/ml of M-CSF (R&D). They were also differentiated into dendritic cells by culturing in the presence of 5 ng/ml of GM-CSF + 5 ng/ml of IL-4 (R&D) or 5 ng/ml of GM-CSF + 1500 units/ml of IFN-α (Biosource International, Camarillo, CA) for 7 days.

3. Results

A small subset of granulocytes was reproducibly shown to have normal ROB activity in both Patient 1 and Patient 2, while the majority of the cells had deficient activity (Fig. 1a). Normal surface gp91^{phox} expression was also reproducibly detected in a small subset of granulocytes from both patients (Fig. 1b), indicating that the granulocytes with normal ROB activity were gp91^{phox}-positive. Subsets of cells with normal ROB activity or normal surface gp91^{phox} expression were not detected in 10 other X-CGD patients studied (Figs. 1a, b, and data not shown). Direct sequence analysis of the *CYBB* gene using genomic DNA from whole blood cells demonstrated a novel c.667 G>T (p.Gly223X) mutation in exon 6 in Patient 1 (Fig. 2a) and a previously reported c.1384 G>T (p.Glu462X) mutation in exon 11 in Patient 2 (Fig. 2b) (Gérard et al., 2001). Mothers of the two patients had only the wild-type sequences of *CYBB* (data not shown), indicating that both patients had *de novo* mutations. However, wild-type sequences at the mutation sites were detected by direct sequencing of PCR products from genomic DNA from both patients after gp91^{phox}-positive granulocytes were enriched with MACS sorting (Figs. 2a and b). The presence of the wild-type sequences was confirmed by sequence analysis of TA clones obtained from gp91^{phox}-positive granulocytes (Figs. 2a and b). These results indicate that a small subset of granulocytes in both patients have the wild-type *CYBB* sequence. Wild-type TA clones of PCR products from genomic DNA were also detected in unselected granulocyte, PBMC, and buccal swab samples from Patient 2, and from a buccal swab sample from Patient 1 (Table 1).

We then studied gp91^{phox} expression and *CYBB* sequences in EBV-LCLs, which are also known to express gp91^{phox}. Although a gp91^{phox}-positive population in EBV-LCLs was not detected 3 weeks after EBV infection, but was detected in a small subset 2 months after its infection in both patients (Fig. 3). This subset, for unknown reasons, was greater

Table 1
Summary of the proportion of granulocytes with normal ROB activity and the proportion of clones with wild-type CYBB sequence in various samples from the two patients.

	Patient 1	Patient 2
ROB + granulocytes	0.9%	3.7%
Wild-type *CYBB* clones		
Granulocytes	0% (0/211)	7.3% (4/55)
PBMC	0% (0/52)	1.6% (1/61)
Buccal swab	1.8% (2/109)	18.8% (6/32)

The fraction in each parenthesis indicates the number of wild-type clones out of the total number of clones analyzed for each sample.

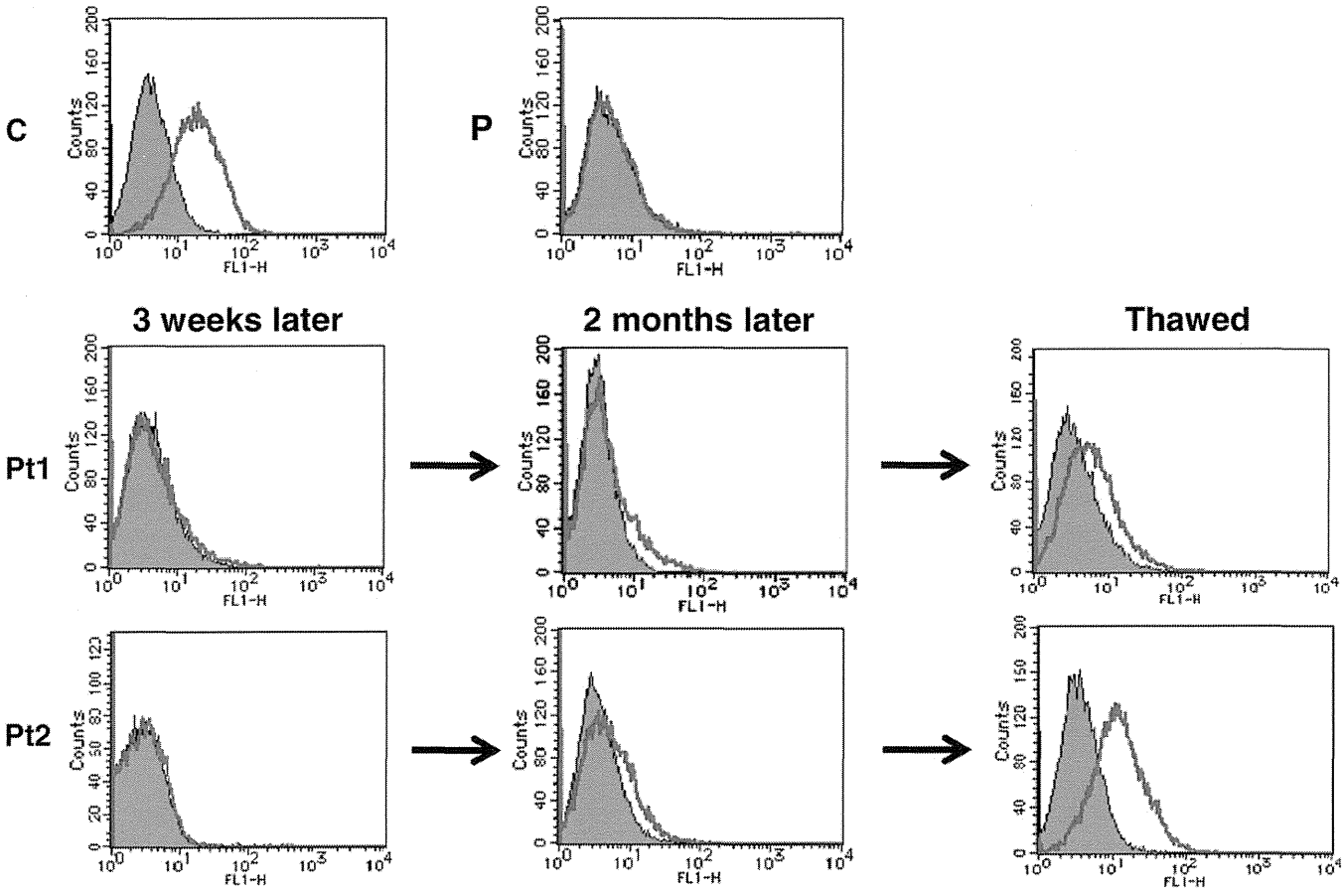

Fig. 3. Surface gp91^{phox} expression in EBV-LCLs 3 weeks and 2 months after EBV infection (3 weeks later and 2 months later). We also studied its expression after thawing the freeze-stored cell lines. Filled orange: isotypic control (mouse IgG1), Empty blue: gp91^{phox} expression.

in some of the EBV-LCLs which were thawed from the freeze-stored original cell lines (Fig. 3 and data not shown). According to the intensity of the wild-type sequence signals, this population was estimated to be about 50% in Patient 1 and 100% in Patient 2, respectively (Fig. 2c).

To exclude the possibility that the normal cells observed in both patients were due to maternal cell engraftment, fluorescent *in situ* hybridization (FISH) analysis of chromosomes X and Y and HLA DNA typing study were performed. FISH analysis in whole blood cells from both patients showed only the XY karyotype in 500 analyzed cells (data not shown). HLA DNA typing also showed only the patients' HLA types of HLA-A*1101, HLA-A*2402, HLA-B*1301, and HLA-B*4002 in enriched gp91^{phox}-positive granulocytes and EBV-LCLs described in Fig. 2c (Table 2). These results indicate that the normal cells were of the patient origin.

CYBB mutations that selectively affect macrophages were recently reported to predispose patients to tuberculous mycobacterial disease (Bustamante et al., 2011), suggesting human tissue macrophages are critical for immunity at least to tuberculosis. To estimate the normal population in tissue macrophages and to study the possibility of selectively expanding the normal population with cytokines, we studied gp91^{phox} expression in monocyte-derived macrophages from Patient 2. Monocyte-derived dendritic cells were also studied. After 7 days of culture, monocytes morphologically changed into macrophages in the presence of GM-CSF or M-CSF, and into dendritic cells in the presence of GM-CSF + IL-4 or GM-CSF + IFNα. The differentiated cells were harvested for the analysis of surface gp91^{phox} expression. Macrophages from normal individuals differentiated with GM-CSF or M-CSF, and dendritic cells differentiated with GM-CSF + IFNα were shown to have surface gp91^{phox} expression comparable to undifferentiated monocytes, while dendritic cells from the normal individuals differentiated with GM-CSF + IL-4 lost its surface expression (data not shown). In Patient 2, the proportions of gp91^{phox} + cells in macrophages differentiated with GM-CSF or M-CSF, and in dendritic cells differentiated with GM-CSF + IFNα, were not significantly different from that of undifferentiated monocytes (Fig. 4).

4. Discussion

This study demonstrates the presence of somatic mosaicism in two unrelated X-CGD patients with *de novo* nonsense mutations in the *CYBB* gene. A small subset of normal cells was found to be present in granulocytes, buccal swab samples, EBV-LCLs, and/or PBMC from both patients.

Somatic mosaicism can result from *de novo* mutations during embryogenesis or from reversion of inherited mutations (Hirschhorn,

Table 2
Results of HLA DNA typing in granulocytes and EBV-LCL.

Sample	A*	A*	B*	B*
Patient 1 granulocytes	1101 (11)	2402 (24)	1301 (13)	4002 (61)
Patient 1 EBV-LCL	1101 (11)	2402 (24)	1301 (13)	4002 (61)
Patient 1's mother granulocytes	2402 (24)	2603 (26)	3501 (35)	4002 (61)
Patient 2 granulocytes	3101 (31)	3303 (33)	4403 (44)	5101 (51)
Patient 2 EBV-LCL	3101 (31)	3303 (33)	4403 (44)	5101 (51)
Patient 2's mother granulocytes	0206 (2)	3303 (33)	4006 (61)	4403 (44)

Enriched gp91^{phox}-positive granulocytes and EBV-LCL were studied for Patient 1 and Patient 2.
( ) : Serotype.

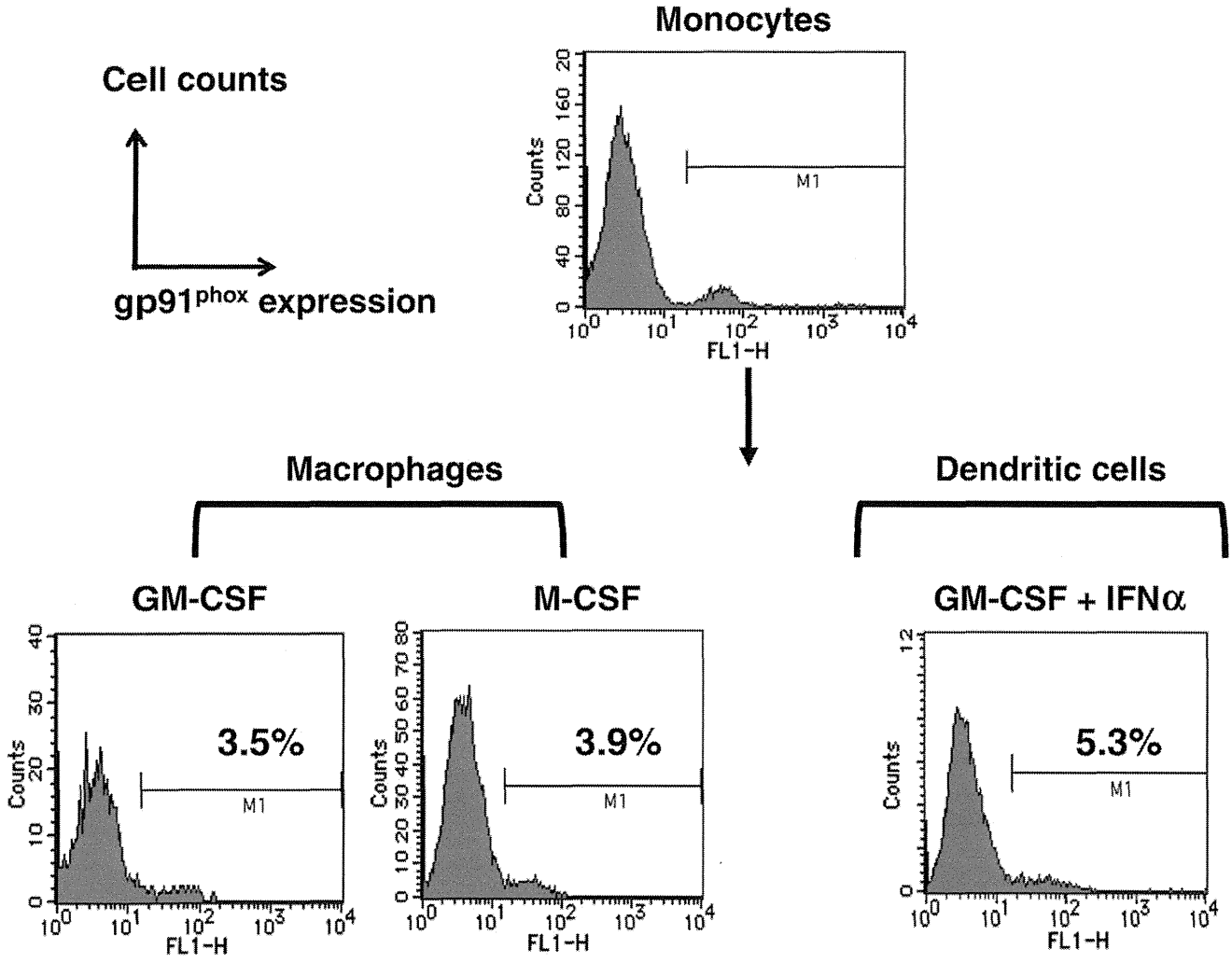

Fig. 4. Surface gp91^{phox} expression in monocytes and monocyte-derived macrophages and dendritic cells in Patient 2. Monocytes were differentiated into macrophages and dendritic cells by the cytokines indicated above each histogram.

2003). A *de novo* mutation could make a significant contribution to the fetus if the mutation occurred at an early stage of embryogenesis, when only a few cells contribute to the embryo (Erickson, 2010). A mutation during embryogenesis may also result in germ line mosaicism depending on the stage of embryogenesis in which the mutation occurs (Frank, 2010; Hirschhorn, 2003). On the other hand, the reversion of inherited mutations has been reported in some disorders, including several PIDs, when the reversion gives a growth advantage to the corrected cells (Hirschhorn, 2003). In these cases the mutation that has reverted to normal has been inherited from a parent (Hirschhorn, 2003).

Considering that the *CYBB* mutations were not detected in their mothers, it is likely that the *de novo* mutations occurred in the patients at an early multicellular stage of embryogenesis with subsequent expansion of the mutated cells, leaving some unmutated cells surviving. This mechanism may also explain the presence of a normal population in various cell lineages as observed in the present patients, since most of the stem cells could carry a mutation when the mutation arises in pluripotent stem cells at an early stage of embryogenesis (Frank, 2010). It might be also possible that the mutations had occurred in oogenesis, and were reverted to normal in a small subset of cells in early embryogenesis. Additionally, we have not completely ruled out the possibility that their mothers have germ line mosaicism and the patients had reversion to normal of inherited mutations in a small subset of cells, although the patients have not had siblings who share the same mutations. In any case, it was not determined whether somatic mosaicism observed in the patients was accompanied by germ line mosaicism in this study.

Somatic mosaicism was observed in leukocytes from an adult female who showed unusual late presentation of X-CGD (Wolach et al., 2005). In contrast, there have been no previous reports of somatic mosaicism in male patients with X-CGD that has been defined at the molecular level, although X-CGD is one of the most common PIDs. Reports of mosaicism in X-CGD may be rare because of the difficulty of detecting a small population of normal cells. Unmutated (revertant) normal cells may have no growth advantage over mutated cells. In fact, Patient 1 was retrospectively shown to have 0.5–1% of granulocytes with normal ROB activity at the age of 3 and 11 years, which had been overlooked until this study. Another possibility is that somatic mosaicism, regardless of its mechanism, is very rare in X-CGD. There is one report of three adult males in two kindreds with X-CGD that was inherited from their mothers, who were shown to have 5–15% of neutrophils and monocytes with normal ROB activity (Woodman et al., 1995). It is possible that these are X-CGD patients with somatic mosaicism, due to reversion of maternally inherited mutations, but the molecular characteristics of the normal cells were not determined in this study, nor was it shown that the normal cells were of patient and not maternal origin.

Somatic mosaicism may have some effects on the clinical phenotype in patients with other PIDs (Ariga et al., 2001a, 2001b; Stephan et al., 1996; Tone et al., 2007; Wada et al., 2001). In X-CGD, based

on studies of female carriers with skewed X-inactivation (Lun et al., 2002; Rösen-Wolff et al., 2001; Wolach et al., 2005), it is estimated that if more than 5–10% of granulocytes are normal, there is much less susceptibility to infection. In Patient 1, a low fraction (<1%) of normal granulocytes had been stably present since the age of 3 years, but he developed liver abscesses at the age of 12 years. This indicates that his clinical course had not been, and probably will not be, modified by the presence of the normal cells. In contrast, Patient 2 might expect some clinical benefit from the normal cells, which were more abundant. It is uncertain whether the normal cell populations in these patients will increase over time. The results of our *in vitro* studies of expanding the normal population have been discouraging (Fig. 3), but these studies focused on the monocytic cells, and not on the granulocytes, which in any case are terminally differentiated. We need to observe if an expansion of the normal granulocytes or monocytes occurs over time *in vivo* which could be correlated with the improvement of clinical phenotypes.

Conflict of interest statement

The authors have no financial conflicts of interest.

Acknowledgments

This work was supported in part by a grant for Research on Intractable Diseases from the Japanese Ministry of Health, Labor and Welfare. We thank Dr. Nakamura M for providing us with monoclonal mouse anti-gp91^{phox} antibody, 7D5. And we thank Dr. Stewart DM for reviewing the manuscript.

References

Ariga, T., et al., 1998. Genetic analysis of 13 families with X-linked chronic granulomatous disease reveals a low proportion of sporadic patients and a high proportion of sporadic carriers. Pediatr. Res. 44, 85–92.

Ariga, T., et al., 2001a. T-cell lines from 2 patients with adenosine deaminase (ADA) deficiency showed the restoration of ADA activity resulted from the reversion of an inherited mutation. Blood 97, 2896–2899.

Ariga, T., et al., 2001b. Spontaneous in vivo reversion of an inherited mutation in the Wiskott-Aldrich syndrome. J. Immunol. 166, 5245–5249.

Bustamante, J., et al., 2011. Germline CYBB mutations that selectively affect macrophages in kindreds with X-linked predisposition to tuberculous mycobacterial disease. Nat. Immunol. 12, 213–221.

Erickson, R.P., 2010. Somatic gene mutation and human disease other than cancer: an update. Mutat. Res. 705, 96–106.

Frank, S.A., 2010. Somatic evolutionary genomics: Mutations during development cause highly variable genetic mosaicism with risk of cancer and neurodegeneration. Proc. Natl. Acad. Sci. U. S. A. 107, 1725–1730.

Gérard, B., et al., 2001. Characterization of 11 novel mutations in the X-linked chronic granulomatous disease (CYBB gene). Hum. Mutat. 18, 163–166.

Hirschhorn, R., 2003. In vivo reversion to normal of inherited mutations in humans. J. Med. Genet. 40, 721–728.

Hui, Y.F., et al., 1997. Identification of mutations in seven Chinese patients with X-linked chronic granulomatous disease. Blood 88, 4021–4028.

Lun, A., et al., 2002. Unusual late onset of X-linked chronic granulomatous disease in an adult woman after unsuspicious childhood. Clin. Chem. 48, 780–781.

Malech, H.L., Gallin, J.I., 1987. Current concepts: immunology. Neutrophils in human diseases. N. Engl. J. Med. 317, 687–694.

Matute, J.D., et al., 2009. A new genetic subgroup of chronic granulomatous disease with autosomal recessive mutations in p40^{phox} and selective defects in neutrophil NADPH oxidase activity. Blood 114, 3309–3315.

Rösen-Wolff, A., et al., 2001. Increased susceptibility of a carrier of X-linked chronic granulomatous disease (CGD) to *Aspergillus fumigatus* infection associated with age-related skewing of lyonization. Ann. Hematol. 80, 113–115.

Stephan, V., et al., 1996. Atypical X-linked severe combined immunodeficiency due to possible spontaneous reversion of the genetic defect in T cells. N. Engl. J. Med. 335, 1563–1567.

Tone, Y., et al., 2007. Somatic revertant mosaicism in a patient with leukocyte adhesion deficiency type 1. Blood 109, 1182–1184.

Tosato, G., Cohen, J. I., 2007. Generation of Epstein-Barr Virus (EBV)-immortalized B cell lines. Curr. Protoc. Immunol. 76, 7.22.1–7.22.4.

Wada, T., et al., 2001. Somatic mosaicism in Wiskott–Aldrich syndrome suggests *in vivo* reversion by a DNA slippage mechanism. Proc. Natl. Acad. Sci. U. S. A. 98, 8697–8702.

Winkelstein, J.A., et al., 2000. Chronic granulomatous disease. Report on a national registry of 368 patients. Medicine (Baltimore) 79, 155–169.

Wolach, B., et al., 2005. Unusual late presentation of X-linked chronic granulomatous disease in an adult female with a somatic mosaic for a novel mutation in CYBB. Blood 105, 61–66.

Woodman, R.C., et al., 1995. A new X-linked variant of chronic granulomatous disease characterized by the existence of a normal clone of respiratory burst-competent phagocytic cells. Blood 85, 231–241.

Yamada, M., et al., 2000. Genetic studies of three Japanese patients with p22-phox-deficient chronic granulomatous disease: detection of a possible common mutant CYBA allele in Japan and a genotype-phenotype correlation in these patients. Br. J. Haematol. 108, 511–517.

Dig Dis Sci
DOI 10.1007/s10620-012-2239-8

ORIGINAL ARTICLE

Increased Susceptibility to Severe Chronic Liver Damage in CXCR4 Conditional Knock-Out Mice

Atsunori Tsuchiya · Michitaka Imai · Hiroteru Kamimura · Masaaki Takamura · Satoshi Yamagiwa · Tatsuki Sugiyama · Minoru Nomoto · Toshio Heike · Takashi Nagasawa · Tatsutoshi Nakahata · Yutaka Aoyagi

Received: 16 November 2011 / Accepted: 2 May 2012

Abstract
Background The chemokine SDF-1 and its receptor CXCR4 are essential for the proper functioning of multiple organs. In the liver, cholangiocytes and hepatic progenitor cells (HPCs) are the main cells that produce SDF-1, and SDF-1 is thought to be essential for HPC-stimulated liver regeneration.
Aims In this study, CXCR4 conditionally targeted mice were used to analyze the role of SDF-1 in chronically damaged liver.
Methods Chronic liver damage was induced in MxCre CXCR4$^{f/null}$ mice and the control MxCre CXCR4$^{f/wt}$ mice by CCl_4. Serum markers were analyzed to assess liver function and damage, the number of cytokeratin-positive cells as a measure of HPCs, and the extent of liver fibrosis. Additional parameters relating to liver damage, such as markers of HPCs, liver function, MMPs, and TIMPs were measured by real-time PCR.
Results Serum ALT was significantly higher in MxCre CXCR4$^{f/null}$ mice than MxCre CXCR4$^{f/wt}$ mice. The number of cytokeratin-positive cells and the area of fibrosis were also increased in the MxCre CXCR4$^{f/null}$ mice. The expression of mRNAs for several markers related to hepatic damage and regeneration was also increased in the liver of MxCre CXCR4$^{f/null}$ mice, including primitive HPC marker prominin-1, MMP9, TNF-α, and α-SMA.
Conclusions MxCre CXCR4$^{f/null}$ mice were susceptible to severe chronic liver damage, suggesting that SDF-1-CXCR4 signals are important for liver regeneration and preventing the progression of liver disease. Modulation of SDF-1 may therefore be a promising treatment strategy for patients with chronic liver disease.

Keywords SDF-1 · CXCR4 · Chronic liver damage · MMP9 · Liver fibrosis · Hepatic progenitor cells

Abbreviations

SDF-1	Stromal cell-derived factor-1
CXCR4	C-X-C chemokine receptor type 4
HGF	Hepatocyte growth factor
bFGF	Basic fibroblast growth factor
EGF	Epidermal growth factor
OSM	Oncostatin M
HIV	Human immunodeficiency virus
pIpC	Poly(I)-poly(C)
PBS	Phosphate-buffered saline
FACS	Fluorescence-activated cell sorter
FITC	Fluorescein isothiocyanate
PCR	Polymerase chain reaction
ALB	Albumin

A. Tsuchiya (✉) · M. Imai · H. Kamimura · M. Takamura · S. Yamagiwa · M. Nomoto · Y. Aoyagi
Division of Gastroenterology and Hepatology, Graduate School of Medical and Dental Science, Niigata University, 1-757 Asahimachi-dori, Chuo-ku, Niigata 951-8510, Japan
e-mail: atsunori@med.niigata-u.ac.jp

T. Sugiyama · T. Nagasawa
Department of Immunobiology and Hematology, Institute for Frontier Medical Sciences, Kyoto University, 53 Kawahara-cho, Shogoin, Sakyo-ku, Kyoto 606-8507, Japan

T. Heike
Department of Pediatrics, Graduate School of Medicine, Kyoto University, 54 Kawahara-cho, Shogoin, Sakyo-ku, Kyoto 606-8507, Japan

T. Nakahata
Department of Clinical Application, Center for iPS Cell Research and Application, Kyoto University, 54 Kawahara-cho, Shogoin, Sakyo-ku, Kyoto 606-8507, Japan

Published online: 05 June 2012

ALP	Alkaline phosphatase
ALT	Alanine aminotransferase
VEGF	Vascular endothelial growth factor
AFP	α-Fetoprotein
NCAM	Neural cell adhesion molecule
DLK-1	Delta-like 1 homolog
G-6-p	Glucose-6-phosphate
CPS1	Carbamoyl phosphate synthetase 1
cyp	Cytochrome P450
α-SMA	α Smooth muscle actin
TNF-α	Tumor necrosis factor-α
TGF-β	Transforming growth factor-β
MMP	Matrix metalloproteinase
TIMP	Tissue inhibitors of metalloproteinases
GAPDH	Glyceraldehydes-3-phosphate dehydrogenase
TGF	Transforming growth factor

Introduction

The liver has a high regenerative capacity but some severely or chronically damaged livers regenerate poorly despite the presence of numerous hepatic stem/progenitor cells [1, 2]. Liver regeneration from hepatic progenitor cells (HPCs) is stimulated by external factors such as HGF, bFGF, EGF [3, 4], and OSM [5], but also produce their own factors that enhance regeneration, such as stromal cell-derived factor-1 (SDF-1).

SDF-1 is a member of a large family of structurally related chemoattractive cytokines and was first characterized as a growth-stimulating factor for B lymphocyte precursors [6, 7]. The primary physiologic receptor for SDF-1 is CXCR4, a seven-transmembrane receptor coupled to heterotrimeric guanosine triphosphate (GTP)-binding proteins [8, 9]. Mice with a heterozygous SDF-1 or CXCR4 mutation are healthy and fertile. Nagasawa et al. reported that homozygous mutant ($SDF\text{-}1^{null/null}$ or $CXCR4^{null/null}$) embryos were present at the expected ratios until day 15.5 of embryogenesis (E15.5); however, about half the $SDF\text{-}1^{null/null}$ or $CXCR4^{null/null}$ embryos were dead at E18.5 and all neonates died within an hour of birth [8, 9]. Subsequent studies using targeted gene disruption of SDF-1-CXCR4 signals have indicated that this pathway is essential for B lymphocyte development [8], maintenance of the hematopoietic stem cell pool in the bone marrow stromal cell niche [10, 11], cardiac vascular formation [12, 13], vascularization of the gastrointestinal tract [9, 14], branching morphology in the pancreas [15], and cerebellar formation [16–18].

Within the liver, SDF-1 is mainly produced by cholangiocytes and HPCs and is upregulated in response to injury [19, 20]. Thus, SDF-1 is thought to contribute to HPC-mediated liver regeneration. The reported roles of SDF-1 in liver regeneration are oval cell activation through autocrine/paracrine pathways [19, 20], collagen production through activation and expansion of hepatic stellate cells [21], and angiogenesis through the mobilization of hematopoietic cells [22]. As described above, SDF-1 affects a variety of CXCR4-positive target cells and has multiple functions. Thus, comprehensive analysis of whether SDF-1 act on positively or negatively during the liver damage is very important in assessing its potential for medical treatment to promote liver regeneration.

In this study, we employed MxCre $CXCR4^{f/null}$ mice to comprehensively analyze the role of SDF-1-CXCR4 signals in damaged livers. Using this mouse, we can conditionally delete CXCR4 in damaged livers after the administration of poly(I)-poly(C) (pIpC), using MxCre $CXCR4^{f/wt}$ mice as controls. Using this system, we analyzed the role of the SDF-1-CXCR4 pathway in chronic liver damage resulting from treatment with CCl_4.

Materials and Methods

Mice

To get MxCre-$CXCR4^{f/null}$ mice and MxCre-$CXCR4^{f/wt}$ mice, $CXCR4^{f/null}$ mice were crossed with MxCre mice [23]. MxCre mice and $CXCR4^{f/null}$ mice were kind gifts from Professor Rajewsky (Harvard Medical School) and Professor Lichtenberg (University of Cologne), and Professor Nagasawa (University of Kyoto), respectively. The strain of these mice was C57BL/6. In MxCre mice, Cre is expressed after the induction of interferon by administration of pIpC. CXCR4 floxed mice have a LoxP-CXCR4 conditional targeting allele. Twelve MxCre-$CXCR4^{f/wt}$ mice and ten MxCre-$CXCR4^{f/null}$ mice were employed in this experiment. Eight-week-old mice were injected pIpC (400 μg per mouse, eight times at 2-day intervals; Amersham Biosciences, Piscataway, NJ) intraperitoneally to induce cre expression. After pIpC treatment, 6 weeks was allowed for recovery from the bone marrow suppression induced by pIpC injection. Then, 1 μl/gram per body weight of CCl_4 (Wako, Osaka, Japan) dissolved in olive oil (Wako) (1:4) was injected intraperitoneally twice a week for 8 weeks to induce chronic liver damage. Eight weeks after the first injection of CCl_4, the mice were analyzed (Fig. 1). For analysis, approximately 500 μl of blood was collected from each mouse, liver weight (LW) and body weight (BW) were calculated, and the livers were removed for flow cytometric analysis, immunohistochemistry, or RNA extraction. Deletion of the floxed CXCR4 gene in the liver was detected by flow cytometry and real-time PCR. All animal experiments were conducted in accordance with the guidelines of Niigata University.

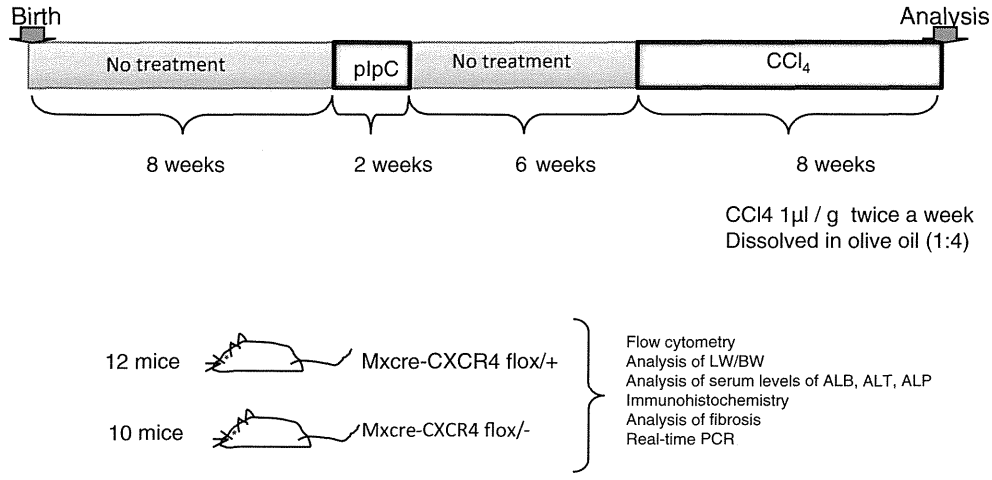

Fig. 1 Summary of experimental approach. MxCre-CXCR4$^{f/null}$ mice and MxCre-CXCR4$^{f/wt}$ mice were employed in this experiment. To delete CXCR4, each mouse was injected with pIpC. After the interval, chronic liver damage was induced by administration of CCl_4. Flow cytometry, analysis of LW/BW, analysis of serum levels of ALB, ALT and ALP, immunohistochemistry, analysis of fibrosis, and real-time PCR were performed to assess the effects of CXCR4 deletion on liver damage

Flow Cytometric Analysis

For flow cytometric analysis, Liver Perfusion Medium (Invitrogen, Carlsbad, CA) and Liver Digest Medium (Invitrogen) were directly injected into the liver. The livers were then minced in 10 ml of Liver Digest Medium and dissociated by gentle MACS® (Miltenyi Biotec, Inc., Auburn, CA). Following dissociation, an equivalent amount of PBS was added and the resulting cell suspension was strained through 70- and 45-μm Cell Strainers (Becton–Dickinson, San Jose, CA), followed by centrifugation at 500 rpm for 1 min to remove centrifuged hepatocytes. The supernatant was centrifuged at 1,000 rpm for 3 min and the centrifuged cells were collected and analyzed using a FACScan (Becton–Dickinson). The antibodies used were FITC conjugated anti-CD45, FITC conjugated anti-CD3, FITC conjugated anti-CD11b, and FITC conjugated anti-CD19 (Becton–Dickinson).

Immunohistochemistry

SDF-1 immunohistochemistry was performed on CCl_4-damaged liver from MxCre-CXCR4$^{f/wt}$ mice and chronic-damaged human liver. For cytokeratin immunohistochemistry, CCl_4 damaged livers of MxCre-CXCR4$^{f/null}$ mice and MxCre-CXCR4$^{f/wt}$ mice were employed. Liver tissue was fixed in 10 % formalin and embedded in paraffin blocks. Four-micrometer sections were cut and mounted on silane-coated slides. For immunohistochemical analysis, paraffin was removed and antigen retrieval was performed using antigen retrieval solution for anti-SDF-1 (BioGenex Laboratories, San Ramon, CA) for 15 min in a microwave oven or using proteinase K for anti-cytokeratin. Endogenous peroxidase activity was blocked with 3 % hydrogen peroxide in methanol (Wako) for 10 min at room temperature, and sections were incubated overnight with the primary antibody, mouse anti-SDF-1 antibody (R&D Systems, Inc., Minneapolis, MN), or anti-cytokeratin antibody that can detect bile duct and hepatic progenitor cells (Dako, Glostroup, Denmark) diluted in PBS. Slides were then stained using the Vectastain® ABC kit (Vector Laboratories, Inc., Burlingame, CA) and DAB TRIS tablets (Muto Pure Chemicals, Tokyo, Japan). Anti-cytokeratin-positive cells that located deep in the lobule and did not form part of ducts were counted. We counted 20 randomly selected fields/screen at 100× magnification.

Real-Time PCR

Total RNA was isolated from the livers using the RNeasy Mini kit (Qiagen, Chatsworth, CA) according to the manufacturer's protocol; 1 μg of total RNA was used as a template for the synthesis of cDNA using the Transcriptor First Strand cDNA Synthesis kit (Roche Applied Science, Mannheim, Germany). Aliquots of cDNA were subjected to real-time PCR using a LightCycler System (Roche Applied Science). The TaqMan probe and primer sets were purchased from Applied Biosystems (Foster City, CA) (Table 1). PCR conditions were as follows: 95 °C for 10 min followed by 45 cycles of 95 °C for 10 s, 60 °C for 30 s, and 72 °C for 1 s. The results were normalized to the level of mRNA for human glyceraldehyde-3-phosphate dehydrogenase (GAPDH).

Analysis of Fibrosis

Formalin-fixed liver sections were stained with Picrosirius Red Stain Kit (Polysciences, Inc. Warrington, PA). Sirius

Table 1 Name of TaqMan probe and primer sets and their assay identification number

Name	Identification number
CXCR4	Mm01292123_m1
SDF-1	Mm00445553_m1
Prominin-1	Mm01211408_m1
AFP	Mm00431715_m1
NCAM	Mm01149710_m1
DLK-1	Mm00494477_m1
α-SMA	Mm01546133_m1
TNF-α	Mm99999068_m1
TGF-β	Mm01178820_m1
TIMP1	Mm00441818_m1
TIMP3	Mm00441827_m1
MMP2	Mm00439491_m1
MMP9	Mm00442991_m1
MMP13	Mm00439491_m1
MMP14	Mm01318966_m1

Red staining was quantitated by ImageJ software in three randomly selected fields/section at 100× magnification.

Statistics

Statistical analyses were performed using GraphPad Prism 5 software (GraphPad Software, Inc., La Jolla, CA). The results were assessed using the Mann–Whitney test. Differences were considered significant when the p value was less than 0.05.

Results

Induced Deletion of CXCR4 in Adult Mouse Livers

The presence of SDF-1-producing cells in mouse and human liver was confirmed by immunohistochemistry. As previously reported, SDF-1-producing cells were located in the bile ducts and cells of ductular reaction that were thought to include HPCs (Fig. 2a, b) [19, 20]. The staining pattern was common between human and mice. Deletion of CXCR4 was confirmed by flow cytometry using liver hematopoietic cells and real-time PCR using liver tissues. In five of the ten MxCre-CXCR4$^{f/null}$ mice, the frequency of CD19+ B lymphocytes in CD45+ hematopoietic cells was significantly reduced (Fig. 2c) and the frequency of CD11b+ monocyte in CD45+ cells was significantly increased (Fig. 2d) in comparison to MxCre-CXCR4$^{f/wt}$ mice. The frequency of CD3+ T cells in CD45+ hematopoietic cells was also increased but this was not statistically significant (Fig. 2e). SDF-1 was first characterized as a pre-B-lymphocyte growth stimulation factor and is essential for B lymphocyte development [6, 7]. Thus, our results suggest that in five of ten MxCre-CXCR4$^{f/null}$ mice, CXCR4 was efficiently deleted. CXCR4 mRNA expression in the liver of these five CXCR4-deleted mice was significantly lower than in MxCre-CXCR4$^{f/wt}$ mice (Fig. 2f). Thus, these five MxCre-CXCR4$^{f/null}$ mice were used for further analysis. No significant differences in SDF-1 mRNA expression were detected between MxCre-CXCR4$^{f/wt}$ and MxCre-CXCR4$^{f/null}$ mice (Fig. 2g).

The Serum Levels of ALT in MxCre-CXCR4$^{f/null}$ Mice Were Significantly Higher Than in MxCre-CXCR4$^{f/wt}$ Mice

To analyze liver damage by CCl_4 in MxCre-CXCR4$^{f/wt}$ mice and MxCre-CXCR4$^{f/null}$ mice, we measured LW/BW, serum levels of ALB, ALT, and ALP. There were no significant differences in LW/BW between the two groups (Fig. 2g). There were no significant difference in the serum levels of ALB and ALP (Fig. 2h, i), but serum ALT was significantly higher in MxCre-CXCR4$^{f/null}$ mice (3,306 ± 5,327 IU/l) than in MxCre-CXCR4$^{f/wt}$ mice (463 ± 323 IU/l) (Fig. 2j), which suggests that there is severe liver damage in the MxCre-CXCR4$^{f/null}$ mice.

The Number of Hepatic Stem/Progenitor Cells was Increased in MxCre-CXCR4$^{f/null}$ Mice

HPCs were enumerated using an anti-cytokeratin antibody, which stains bile duct and HPCs. The number of anti-cytokeratin-positive cells in MxCre-CXCR4$^{f/null}$ mice (159.1 ± 48.7 cells/field) was significantly higher than in MxCre-CXCR4$^{f/wt}$ mice (81.8 ± 32.2 cells/field) (Fig. 3a–c). To detect altered expression of HPC markers in conditional CXCR4-deleted mice, mRNA levels of prominin-1, AFP, NCAM, and DLK-1 were measured. The mRNA levels of AFP and particularly of prominin-1 were increased in the liver of MxCre-CXCR4$^{f/null}$ mice, while the levels of NCAM and DLK-1 were not affected by CXCR4 targeting (Fig. 3d–g). Prominin-1 is a primitive hepatic stem/progenitor marker [2, 24], and these results therefore suggest that activation of hepatic stem/progenitor cells occurred more strongly in MxCre-CXCR4$^{f/null}$ mice than in MxCre-CXCR4$^{f/wt}$ mice.

Increased Liver Fibrosis in MxCre-CXCR4$^{f/null}$ Mice

Liver fibrosis in tissue sections was analyzed by Sirius Red staining, which identifies areas of collagen accumulation. The extent of Sirius Red staining was significantly higher in the liver of MxCre-CXCR4$^{f/null}$ mice (2.7 ± 0.6 %) than in MxCre-CXCR4$^{f/wt}$ mice (1.6 ± 0.5 %) (Fig. 4a–c). To confirm our results, mRNA expression of a range of markers of liver fibrosis were measured; mRNA of stellate cell

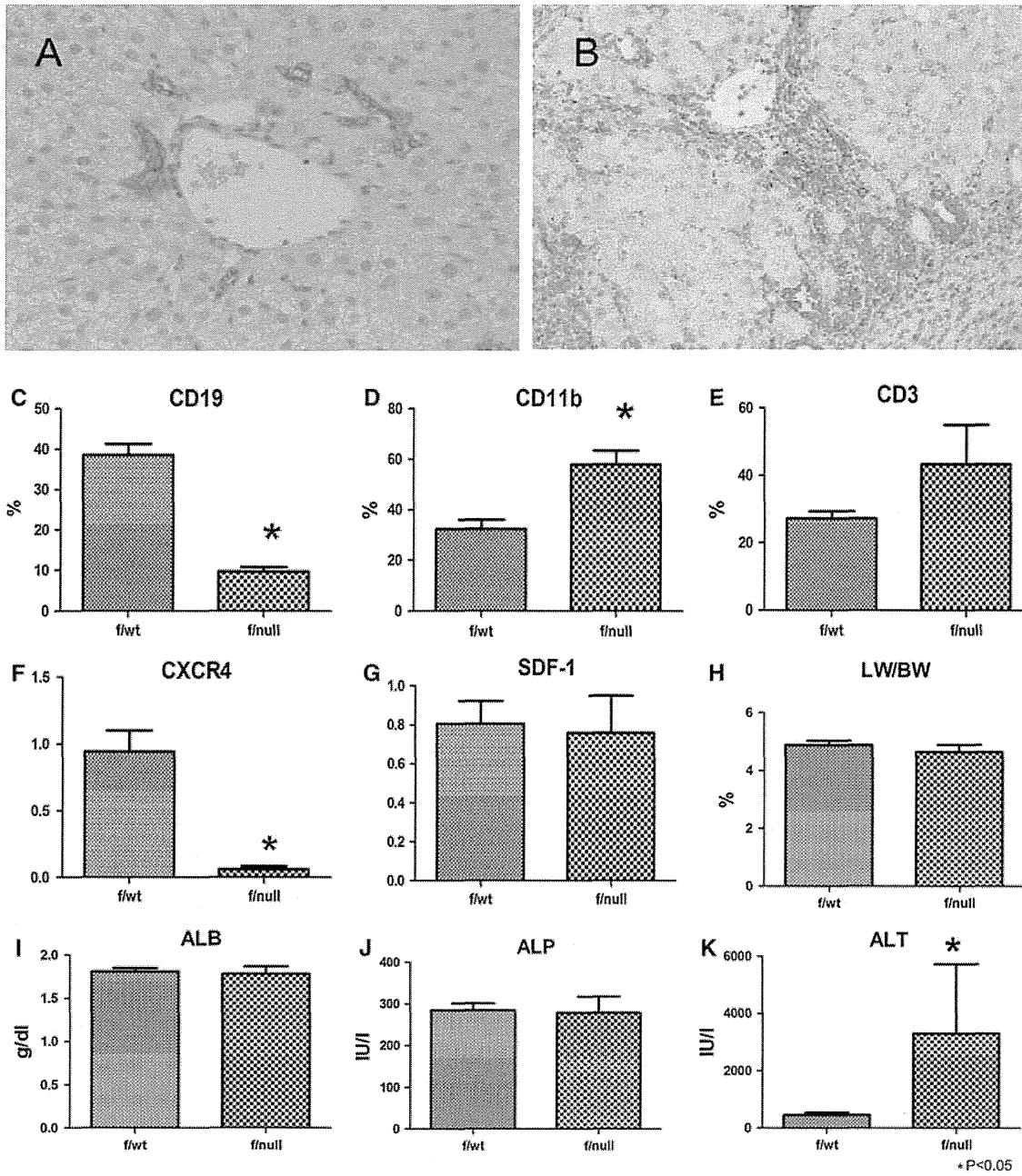

Fig. 2 Immunohistochemistry for SDF-1 (**a**, **b**), flow cytometric analysis of hematopoietic cells in the liver (**c**–**e**), and analysis of CXCR4 and SDF-1 mRNA in the liver (**g**, **f**). In both the mouse (**a**) and human (**b**) livers, cholangiocytes and HPCs express SDF-1. Flow cytometric analysis of CD19 (**c**), CD11b (**d**), and CD3 cells (**e**) in CD45 cells revealed that CD19 cells were significantly decreased and CD11b and CD3 cells were increased in five of ten MxCre-CXCR4$^{f/null}$ mice. Real-time PCR analysis revealed that in these five mice, although the mRNA of SDF-1 was not different (**g**), the mRNA levels of CXCR4 were significantly decreased (**f**). Analysis of LW/BW (**h**) and serum levels of liver markers (**i**–**k**). LW/BW was not different between the two groups (**h**). The serum levels of ALB (**i**), ALP (**j**) were not different, but the serum levels of ALT (**k**) in MxCre-CXCR4$^{f/null}$ mice were significantly higher than in MxCre-CXCR4$^{f/wt}$ mice

markers (α-SMA, TNF-α, and TGF-β), the mRNA levels of MMPs (MMP2, MMP9, MMP13, and MMP14) and the mRNA levels of TIMPs (TIMP1 and TIMP3). The expression of α-SMA and TNF-α mRNA was significant higher in MxCre-CXCR4$^{f/null}$ mice than in MxCre-CXCR4$^{f/wt}$ mice (Fig. 4d, e), while the expression of TGF-β mRNA was not changed (Fig. 4f). These results suggest enhanced activation of some signals of stellate cells in the liver of MxCre-CXCR4$^{f/null}$ mice. In the mRNA levels of the MMPs, the mRNA of MMP9 was significantly increased in the liver of MxCre-CXCR4$^{f/null}$ mice (Fig. 4g–j). There were no differences in expression of the TIMP mRNAs between the two

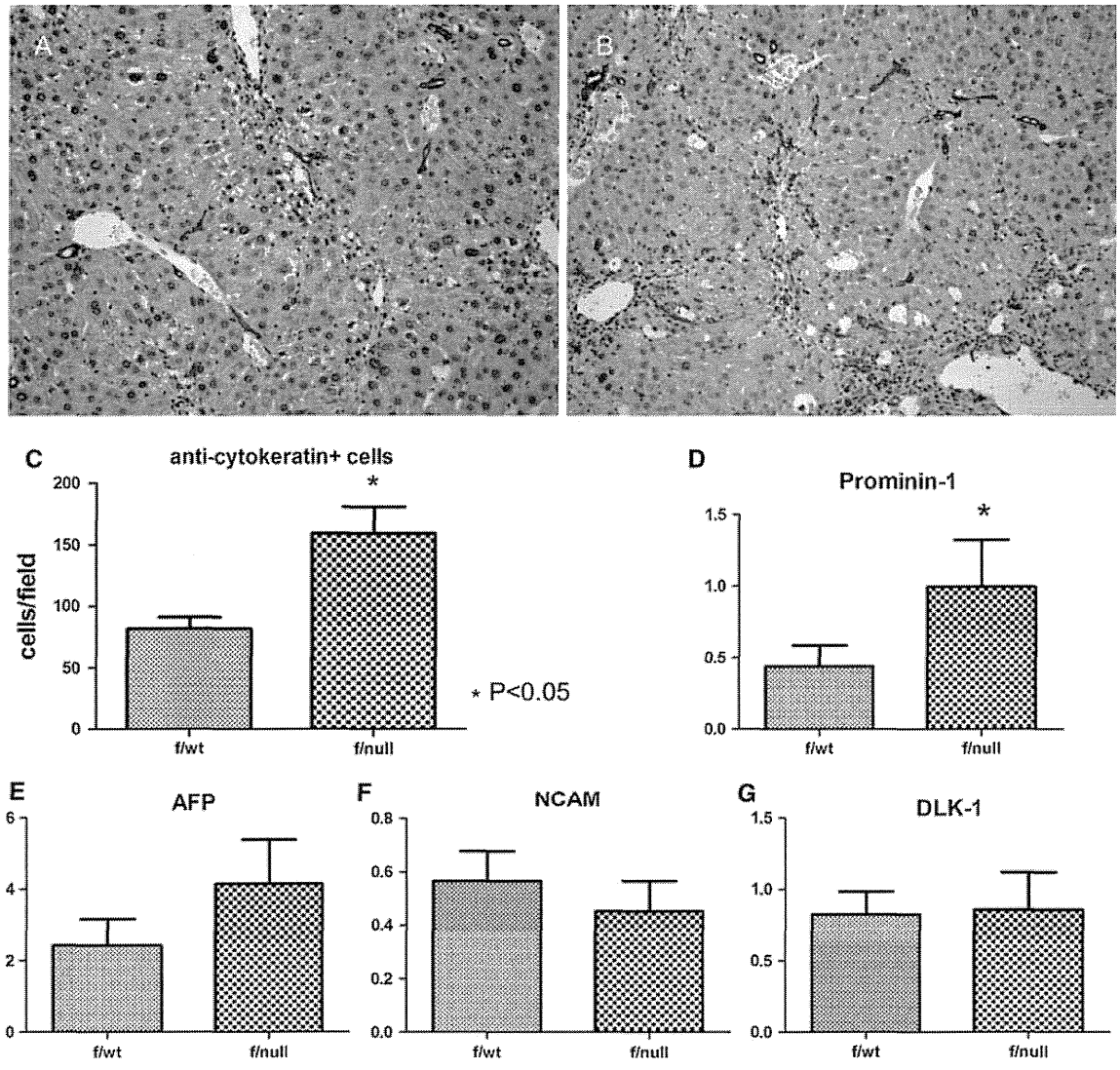

Fig. 3 Immunohistochemistry for detection of cytokeratin-positive cells (**a**–**c**) and real-time PCR analysis of HPC markers (**d**–**g**). Analysis of MxCre-CXCR4$^{f/wt}$ mice (**a**) and MxCre-CXCR4$^{f/null}$ mice (**b**) revealed that the number of cytokeratin-positive cells in the liver of MxCre-CXCR4$^{f/null}$ mice was significantly higher than in MxCre-CXCR4$^{f/wt}$ mice (**c**). Analysis of HPC markers revealed that mRNA expression of the most primitive HPC marker prominin-1 was significantly higher in MxCre-CXCR4$^{f/null}$ mice (**d**). AFP mRNA expression was higher in MxCre-CXCR4$^{f/null}$ mice, but the difference was not significant (**e**). The mRNA levels of NCAM (**f**) and DLK-1 (**g**) were not affected by CXCR4 targeting

groups (Fig. 4k, l). The activation of some signals of stellate cells and up-regulation of the MMP9 mRNA in MxCre-CXCR4$^{f/null}$ mice are consistent with the results suggesting severe liver damage in the MxCre-CXCR4$^{f/null}$ mice.

Discussion

Previous reports have shown that SDF-1-CXCR4 signals are essential for the function of multiple organs such as bone marrow [6–8, 10, 11], brain [16–18], heart [12, 13], and blood vessels [9, 14]. However, the contribution of SDF-1-CXCR4 signals to the pathogenesis of chronic liver damage is not known. In this study, we analyzed the role of SDF1-CXCR4 signals in CCl_4-induced chronic liver damage in CXCR4 conditionally targeted mice. MxCre-CXCR4$^{f/null}$ mice suffered enhanced liver damage compared with MxCre-CXCR4$^{f/wt}$ mice. Furthermore, the number of HPCs was increased in the liver of MxCre-CXCR4$^{f/null}$ mice, but the HPCs did not appear to undergo full differentiation and liver fibrosis was severe. We conclude that SDF-1-CXCR4 signaling contributes to hepatic protection and liver regeneration.

Several previous studies have analyzed SDF-1-CXCR4 signals in the liver; however, their conclusions varied somewhat from our study. Mavier et al. reported that SDF-1 stimulates the proliferation of HPCs through an autocrine/paracrine pathway [19] and Zheng et al. reported

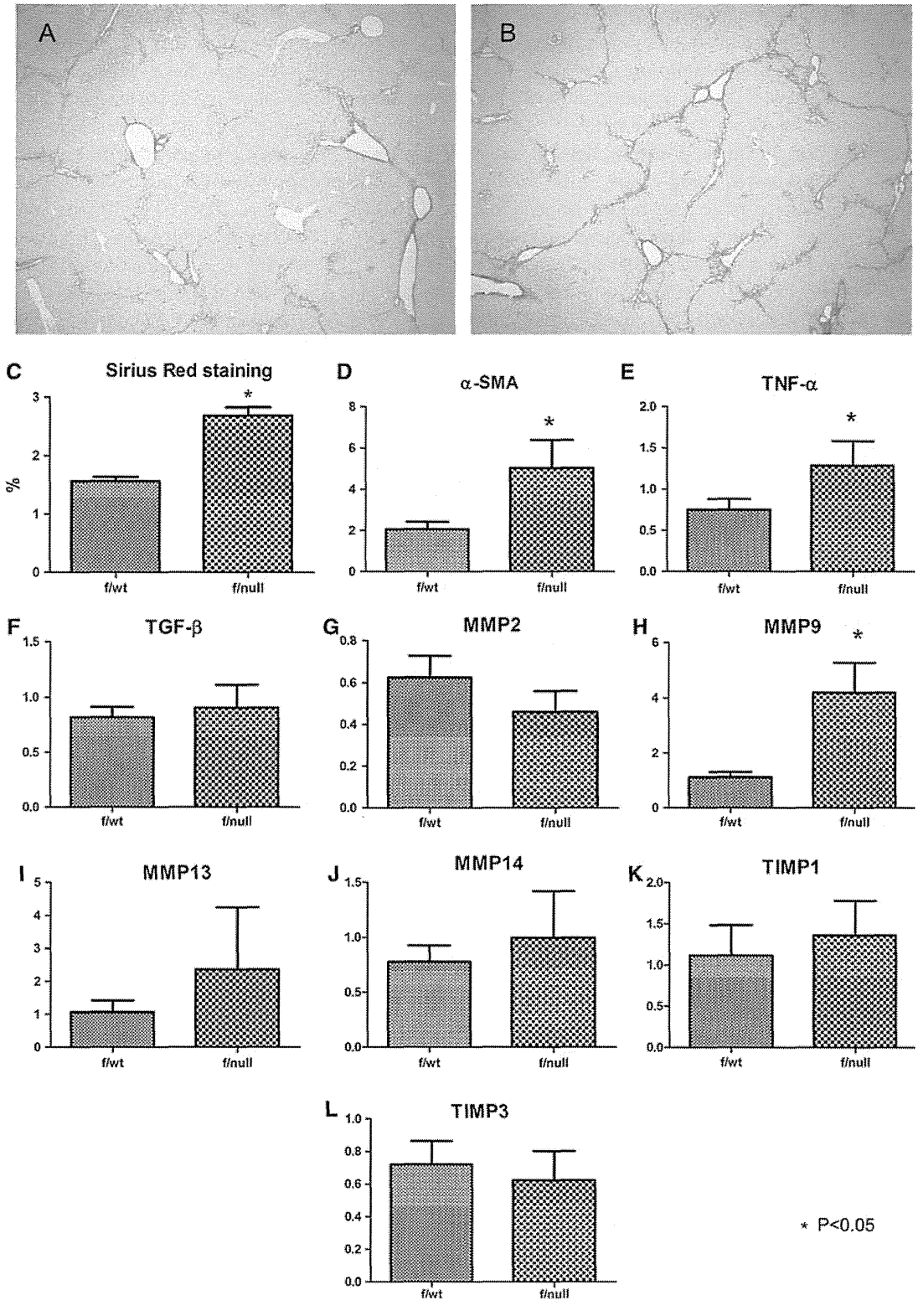

Fig. 4 Analysis of fibrosis by Sirius Red staining (**a–c**) and real-time PCR analysis of hepatic stellate cells markers, TIMPs, and MMPs (**d–l**). Sirius Red staining of MxCre-CXCR4$^{f/wt}$ (**a**) and MxCre-CXCR4$^{f/null}$ mice (**b**) revealed that the extent of the area of fibrosis (*red area*) in MxCre-CXCR4$^{f/null}$ mice was significantly higher than in MxCre-CXCR4$^{f/wt}$ mice (**c**). The mRNA levels of α-SMA and TNF-α were significant higher in the livers of MxCre-CXCR4$^{f/null}$ mice than in MxCre-CXCR4$^{f/wt}$ mice (**d**, **e**) but the mRNA levels of TGF-β were not different (**f**). The mRNA levels of MMP2 (**g**), MMP13 (**i**), MMP14 (**j**), TIMP1 (**k**) and TIMP3 (**l**) were not different, but the mRNA level of MMP9 (**h**) was significantly higher in the MxCre-CXCR4$^{f/null}$ mice than in the MxCre-CXCR4$^{f/wt}$ mice

that SDF-1 is essential for activation of HPCs [20]. Our analysis revealed that the number of cytokeratin-positive cells, which includes hepatic stem/progenitor cells, was increased in the liver of CXCR4 conditionally deleted mice. Furthermore, expression of prominin-1 mRNA, which is a marker for the most primitive hepatic stem/progenitor cells, was increased significantly in the liver of CXCR4 conditional deleted mice. Our results suggest that SDF-1-CXCR4 signals promote liver regeneration. The difference between our study and the studies of Zheng et al. and Mavier et al. may be due to differences in the animal models or drugs used. We consider that mice with CXCR4 targeted specifically in hepatic stem/progenitor cells will be very valuable in resolving these issues.

Hong et al. reported that SDF-1-CXCR4 signals are important for HSC activation, fibrogenesis, and proliferation [21]. These authors also suggested that small molecular inhibitors of CXCR4 may have antifibrotic properties. However, in our study, liver fibrosis was exacerbated in CXCR4 conditionally deleted mice, which was further confirmed by the up-regulation of mRNAs for MMP9, TNF-α, and α-SMA. Thus, our results indicate that SDF-1-CXCR4 signals are important for preventing the progression of liver fibrosis, and that blocking this pathway may not be a safe strategy for the treatment of liver damage.

Glunwald et al. reported that SDF-1 is important for retention of a pro-angiogenic subpopulation of hematopoietic cells in the liver [22]. One caveat to our study is the differing hematopoietic cell populations in the MxCre-CXCR4$^{f/null}$ and MxCre-CXCR4$^{f/wt}$ mice; the MxCre-CXCR4$^{f/null}$ mice have a reduction in B lymphocyte number and a slight increase in monocytes in the liver. We cannot exclude the possibility that the differences in the hematopoietic cells populations influenced the results. However, CXCR4 is expressed by multiple cell types, and it is not currently possible to specifically target CXCR4 on specific cells. Nonetheless, our study clearly suggests that SDF-1-CXCR4 signals are important in liver regeneration and hepatic protection.

In our study, CXCR4 was effectively deleted in MxCre-CXCR4$^{f/null}$ mice, however the mRNA of SDF-1 was not different between the two groups. Kojima et al. reported that SDF-1 affect the production of SDF-1 by feed-forward manner [25]. Thus we think that although MxCre-CXCR4$^{f/null}$ mice had more anti-cytokeratin-positive cells, the production of SDF-1 per cell was lower in MxCre-CXCR4$^{f/null}$ mice.

It may be possible to exploit our findings to develop new treatments to promote liver regeneration. SDF-1-CXCR4 signals can be modulated by external factors. Leucocyte-derived protease or cell-surface-expressed CD26/dipeptidylpeptidase IV (DPPIV) can cleave both SDF-1 and the N-terminus of CXCR4 [26], and DPPIV activity is known to be increased in chronically damaged livers [27]. Therefore, protease inhibitors may have value for preventing the cleavage of SDF-1 and CXCR4 in the liver. DPPIV inhibitors have already been widely used to treat type 2 diabetes mellitus, and they may also promote liver regeneration and hepatic protection by preventing the cleavage of SDF-1 and CXCR4. Furthermore, SDF-1-CXCR4 signals can be modulated by a broad range of mediators, both positively (e.g., PMV, C3a, des-arg C3a, thrombin, uPAR, fibronectin, hyaluronic acid, sICAM1, and cVCAM1) and negatively (e.g., lipopolysaccharide (LPS), heparin, MIP-1α, and PATENT) [26]. Therefore, modulation of SDF-1 production by HPCs is an additional strategy for stimulation of liver regeneration and hepatic protection.

Acknowledgments We thank Professor Rajewsky (Harvard Medical School) and Professor Lichtenberg (University of Cologne) for providing MxCre mice. This research was supported by Tsukada memorial grant, by a Grant-in Aid for Young Scientists (B, 22790634) of The Ministry of Education, Culture, Sports, Science and Technology and by a Grant for Promotion of Niigata University Research Project.

Conflict of interest None.

References

1. Forbes S, Vig P, Poulsom R, et al. Hepatic stem cells. *J Pathol.* 2002;197:510–518.
2. Tsuchiya A, Kamimura H, Takamura M, et al. Clinicopathological analysis of CD133 and NCAM human hepatic stem/progenitor cells in damaged livers and hepatocellular carcinomas. *Hepatol Res.* 2009;39:1080–1090.
3. Tsuchiya A, Heike T, Fujino H, et al. Long-term extensive expansion of mouse hepatic stem/progenitor cells in a novel serum-free culture system. *Gastroenterology.* 2005;128:2089–2104.
4. Tsuchiya A, Heike T, Baba S, et al. Long-term culture of postnatal mouse hepatic stem/progenitor cells and their relative developmental hierarchy. *Stem Cells.* 2007;25:895–902.
5. Miyajima A, Kinoshita T, Tanaka M, et al. Role of oncostatin M in hematopoiesis and liver development. *Cytokine Growth Factor Rev.* 2000;11:177–183.
6. Nagasawa T, Kaisho T, Kishimoto T, et al. Generation and characterization of a monoclonal antibody that inhibits stromal cell-dependent B lymphopoiesis. *J Immunol.* 1994;152:2788–2797.
7. Nagasawa T, Kikutani H, Kishimoto T. Molecular cloning and structure of a pre-B-cell growth-stimulating factor. *Proc Natl Acad Sci USA.* 1994;91:2305–2309.
8. Nagasawa T, Hirota S, Tachibana K, et al. Defects of B-cell lymphopoiesis and bone-marrow myelopoiesis in mice lacking the CXC chemokine PBSF/SDF-1. *Nature.* 1996;382:635–638.
9. Tachibana K, Hirota S, Iizasa H, et al. The chemokine receptor CXCR4 is essential for vascularization of the gastrointestinal tract. *Nature.* 1998;393:591–594.
10. Tokoyoda K, Egawa T, Sugiyama T, et al. Cellular niches controlling B lymphocyte behavior within bone marrow during development. *Immunity.* 2004;20:707–718.
11. Sugiyama T, Kohara H, Noda M, et al. Maintenance of the hematopoietic stem cell pool by CXCL12-CXCR4 chemokine

signaling in bone marrow stromal cell niches. *Immunity*. 2006;25: 977–988.
12. Cheng Z, Liu X, Ou L, et al. Mobilization of mesenchymal stem cells by granulocyte colony-stimulating factor in rats with acute myocardial infarction. *Cardiovasc Drugs Ther*. 2008;22: 363–371.
13. Sanematsu F, Hirashima M, Laurin M, et al. DOCK180 is a Rac activator that regulates cardiovascular development by acting downstream of CXCR4. *Circ Res*. 2010;107:1102–1105.
14. Ara T, Tokoyoda K, Okamoto R, et al. The role of CXCL12 in the organ-specific process of artery formation. *Blood*. 2005;105: 3155–3161.
15. Hick AC, van Eyll JM, Cordi S, et al. Mechanism of primitive duct formation in the pancreas and submandibular glands: a role for SDF-1. *BMC Dev Biol*. 2009;9:66.
16. Stumm RK, Zhou C, Ara T, et al. CXCR4 regulates interneuron migration in the developing neocortex. *J Neurosci*. 2003;23: 5123–5130.
17. Zhu Y, Yu T, Zhang XC, et al. Role of the chemokine SDF-1 as the meningeal attractant for embryonic cerebellar neurons. *Nat Neurosci*. 2002;5:719–720.
18. Zhu Y, Matsumoto T, Mikami S, et al. SDF1/CXCR4 signalling regulates two distinct processes of precerebellar neuronal migration and its depletion leads to abnormal pontine nuclei formation. *Development*. 2009;136:1919–1928.
19. Mavier P, Martin N, Couchie D, et al. Expression of stromal cell-derived factor-1 and of its receptor CXCR4 in liver regeneration from oval cells in rat. *Am J Pathol*. 2004;165:1969–1977.
20. Zheng D, Oh SH, Jung Y, et al. Oval cell response in 2-acetylaminofluorene/partial hepatectomy rat is attenuated by short interfering RNA targeted to stromal cell-derived factor-1. *Am J Pathol*. 2006;169:2066–2074.
21. Hong F, Tuyama A, Lee TF, et al. Hepatic stellate cells express functional CXCR4: role in stromal cell-derived factor-1alpha-mediated stellate cell activation. *Hepatology*. 2009;49:2055–2067.
22. Grunewald M, Avraham I, Dor Y, et al. VEGF-induced adult neovascularization: recruitment, retention, and role of accessory cells. *Cell*. 2006;124:175–189.
23. Kuhn R, Schwenk F, Aguet M, et al. Inducible gene targeting in mice. *Science*. 1995;269:1427–1429.
24. Rountree CB, Barsky L, Ge S, et al. A CD133-expressing murine liver oval cell population with bilineage potential. *Stem Cells*. 2007;25:2419–2429.
25. Kojima Y, Acar A, Eaton EN, et al. Autocrine TGF-β and stromal cell-derived factor-1 (SDF-1) signaling drives the evolution of tumor-promoting mammary stromal myofibroblast. *Proc Natl Acad Sci USA*. 2010;107:20009–20014.
26. Kucia M, Jankowski K, Reca R, et al. CXCR4-SDF-1 signalling, locomotion, chemotaxis and adhesion. *J Mol Histol*. 2004;35: 233–245.
27. Balaban YH, Korkusuz P, Simsek H, et al. Dipeptidyl peptidase IV (DDP IV) in NASH patients. *Ann Hepatol*. 2007;6:242–250.

ORIGINAL ARTICLE CLINICAL IMMUNOLOGY

Clinical features and outcome of X-linked lymphoproliferative syndrome type 1 (SAP deficiency) in Japan identified by the combination of flow cytometric assay and genetic analysis

Hirokazu Kanegane[1], Xi Yang[1], Meina Zhao[1], Kazumi Yamato[2], Masami Inoue[3], Kazuko Hamamoto[4], Chie Kobayashi[5,6], Ako Hosono[7], Yoshikiyo Ito[8], Yozo Nakazawa[9], Kiminori Terui[10], Kazuhiro Kogawa[11], Eiichi Ishii[12], Ryo Sumazaki[6] & Toshio Miyawaki[1]

[1]Department of Pediatrics, Graduate School of Medicine, University of Toyama, Toyama, Japan; [2]Department of Pediatrics, Graduate School of Medicine, Osaka City University, Osaka, Japan; [3]Department of Hematology/Oncology, Osaka Medical Center and Research Institute for Maternal and Child Health, Izumi, Japan; [4]Department of Pediatrics, Hiroshima Red Cross Hospital and Atomic-bomb Survivors Hospital, Hiroshima, Japan; [5]Department of Pediatrics, Ibaraki Children's Hospital, Mito, Japan; [6]Department of Child Health, Institute of Clinical Medicine, University of Tsukuba, Tsukuba, Japan; [7]Department of Pediatrics, National Cancer Center Hospital, Tokyo, Japan; [8]Department of Hematology, Harasanshin Hospital, Fukuoka, Japan; [9]Department of Pediatrics, Shinshu University Graduate School of Medicine, Matsumoto, Japan; [10]Department of Pediatrics, Hirosaki University Graduate School of Medicine, Hirosaki, Japan; [11]Department of Pediatrics, National Defense Medical College, Tokorozawa, Japan; [12]Department of Pediatrics, Ehime University Graduate School of Medicine, Toon, Japan

To cite this article: Kanegane H, Yang Xi, Zhao M, Yamato K, Inoue M, Hamamoto K, Kobayashi C, Hosono A, Ito Y, Nakazawa Y, Terui K, Kogawa K, Ishii E, Sumazaki R, Miyawaki T. Clinical features and outcome of X-linked lymphoproliferative syndrome type 1 (SAP deficiency) in Japan identified by the combination of flow cytometric assay and genetic analysis. *Pediatric Allergy Immunology* 2012: **23**: 488–493.

Keywords
flow cytometry; genetic analysis; hematopoietic stem cell transplantation; SLAM-associated protein; X-linked lymphoproliferative syndrome

Correspondence
Hirokazu Kanegane, Department of Pediatrics, Graduate School of Medicine, University of Toyama, 2630 Sugitani, Toyama, Toyama 930-0194, Japan
Tel.: 81 76 434 7313
Fax: 81 76 434 5029
E-mail: kanegane@med.u-toyama.ac.jp

Accepted for publication 18 January 2012

DOI:10.1111/j.1399-3038.2012.01282.x

Abstract

Objective: X-linked lymphoproliferative syndrome (XLP) type 1 is a rare immunodeficiency, which is caused by mutations in *SH2D1A* gene. The prognosis of XLP is very poor, and hematopoietic stem cell transplantation (HSCT) is the only curative therapy. We characterized the clinical features and outcome of Japanese patients with XLP-1.

Methods: We used a combination of flow cytometric analysis and genetic analysis to identify XLP-1 and reviewed the patient characteristics and survival with HSCT.

Results: We identified 33 patients from 21 families with XLP-1 in Japan. Twenty-one of the patients (65%) who did not undergo a transplant died of the disease and complications. Twelve patients underwent HSCT, and 11 of these (92%) survived.

Conclusion: We described the clinical characteristics and outcomes of Japanese patients with XLP-1, and HSCT was the only curative therapy for XLP-1. The rapid and accurate diagnosis of XLP with the combination of flow cytometric assay and genetic analysis is important.

X-linked lymphoproliferative syndrome (XLP) is a rare inherited immunodeficiency estimated to affect approximately one in one million males, although it may be under-diagnosed (1). XLP is characterized by extreme vulnerability to Epstein–Barr virus (EBV) infection, and the major clinical phenotypes of XLP include fulminant infectious mononucleosis (FIM) or EBV-associated hemophagocytic lymphohistiocytosis (HLH) (60%), lymphoproliferative disorder (30%), and dysgammaglobulinemia (30%) (2). In addition, XLP is associated with a variety of other clinical manifestations including vasculitis, aplastic anemia, and pulmonary lymphoid granulomatosis. Patients with XLP often develop more than one phenotype over time.

The responsible gene was first identified as *SH2D1A/SLAM-associated protein (SAP)* located in the region of Xq25 (3–5). However, some of the presumed patients with

XLP do not harbor *SH2D1A* mutations, although they are clinically and even histologically similar to XLP patients with *SH2D1A* mutations. A second causative gene that encodes X-linked inhibitor of apoptosis protein (XIAP), namely *XIAP* or *BIRC4* gene, has been identified (6). Patients with XLP-2 (XIAP deficiency) sometimes present with splenomegaly and hemorrhagic colitis, but no lymphoma. The *SH2D1A* and *XIAP* genes are close together at Xq25, but the molecular pathogenesis and clinical features of these diseases seem to be distinct (7, 8).

The vast majority of patients with XLP die in childhood; the survival rate is very poor, even with treatment (2). Hematopoietic stem cell transplantation (HSCT) is the only curative therapy for XLP (9, 10). Therefore, rapid definitive diagnosis and immediate treatment are extremely significant for better prognosis and survival of patients with XLP. We previously established the anti-SAP monoclonal antibody (mAb) and applied it to flow cytometric diagnosis of patients with XLP-1 (11). We performed a nationwide survey for XLP-1 with the flow cytometric assay and genetic analysis and identified a total of 33 patients from 21 families with XLP-1 in Japan (11–15). In this study, we elucidated the clinical and genetic characteristics of these patients. Twelve patients with XLP-1 underwent HSCT, and 11 of these (92%) survived. We also describe the outcomes of HSCT in Japan.

Materials and methods

Study subjects

The subjects in this study were largely male patients with FIM or EBV–HLH treated until the end of 2011. In addition, a few male patients with lymphoma or hypogammaglobulinemia with unknown genetic origin were suspected of having XLP. After written informed consent was obtained, 5–10 ml of venous blood was collected into heparin-containing syringes and delivered to the laboratory. Patients and families provided informed consent for genetic analyses in accordance with the 1975 Declaration of Helsinki, and the study protocol was approved by the Ethics Committee of the University of Toyama. Several patients were described in our previous reports (11–15).

Flow cytometric analysis of SAP

Flow cytometric analysis of SAP was performed as previously described (11, 12). The peripheral blood mononuclear cells (PBMC) were isolated by Ficoll–Hypaque density gradient centrifugation and immediately fixed in 1% paraformaldehyde for 30 min at room temperature and then permeabilized in 0.5% saponin for 15 min on ice. To test the expression of SAP in lymphocytes, these cells were incubated with 2 μg/ml anti-SAP mAb, termed KST-3 (rat IgG1) or irreverent rat IgG1, for 20 min on ice and further stained with a 1:1000 dilution of FITC-labeled goat anti-rat IgG antibody (Zymed, South San Francisco, CA, USA) or Alexa Fluor 488-conjugated goat anti-rat IgG antibody (Molecular Probes, Eugene, OR, USA) for 20 min on ice. To evaluate SAP expression in $CD8^+$ T and NK cells, PBMC were stained with phycoerythrin (PE)-conjugated anti-CD8 and anti-CD56 mAbs (DAKO Japan, Kyoto, Japan), respectively, before cellular fixation and permeabilization. The stained cells were analyzed using a flow cytometer (EPICS XL-MCL; Beckman Coulter KK, Tokyo, Japan).

SH2D1A mutation detection

The *SH2D1A* mutations were detected by direct sequencing as described previously (5, 14). Genomic DNA was purified from PBMC with a QIAamp Blood Kit (Qiagen, Hilden, Germany) and amplified using primers encompassing each exon–intron boundary of the *SH2D1A* genes. The sequencing reaction was carried out using a BigDye Terminator Cycle Sequencing Kit (Applied Biosystems, Foster City, CA, USA) with an automated ABI PRISM 310 DNA sequencer (Applied Biosystems).

Results

SAP expression in patients with XLP-1

Fresh blood cells were available in 19 patients with XLP-1. All the examined patients demonstrated markedly deficient SAP expression in lymphocytes, especially in $CD8^+$ T cells and NK cells (Fig. 1 and Table 1).

SH2D1A mutations

All the mutations including unpublished data are summarized with the clinical data (Table 1). There were three gross deletions (the whole gene and two exons 3 and 4), four nonsense mutations (all Arg55stop), eight missense mutations (Ala3Ser, Tyr7Cys, two His8Asp, Gly27Ser, Asp33Tyr, Ser34Gly and Gly49Val), two small deletions (584delA and 1021delAA), two small insertions (312insG and 545insA), and two splicing anomalies (416C > T and IVS2 + 1G > A). The substitution of 416C with T revealed an aberrantly spliced cDNA with deletion of the last 22 bases of exon 1, and IVS2 + 1G > A resulted in skipping of exon 2.

Clinical characteristics of Japanese patients with XLP-1

Eighteen of the 33 patients (55%) had FIM or EBV–HLH, 12 patients (36%) had hypogammaglobulinemia, seven patients (21%) had malignant lymphoma or lymphoproliferative disease, and two patients (P4.2 and P7.2) had lymphocytic vasculitis. One patient (P7.1) had aplastic anemia. Twenty-seven patients (82%) were associated with EBV infection at the disease onset. Two patients (P16.1 and P19.3) presented with non-EBV–HLH. Interestingly, malignant lymphoma and lymphocytic vasculitis in P4.2 were not associated with EBV infection, but the patient later developed EBV–HLH at the age of 14 yr and died of HLH. Two patients (P17.2 and P21.1) had encephalitis: and P17.2 developed acute disseminated encephalomyelitis caused by human

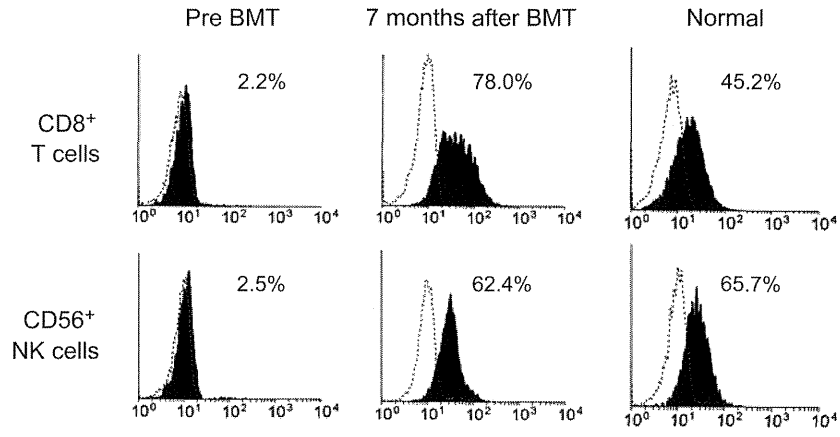

Figure 1 The SAP expression in $CD8^+$ T cells and NK cells from the patient (P16.1) and a normal adult donor. Dotted lines and shaded areas indicate staining by the control antibody and anti-SAP mAb (KST-3), respectively. A flow cytometric analysis demonstrated that deficient SAP expression in $CD8^+$ T cells and NK cells from the patient increased after he had undergone hematopoietic stem cell transplantation.

herpes virus 6 infection and P21.1 developed EBV encephalitis. Approximately 70% of the patients (23 of 33) were diagnosed by the time they were 5 yr of age, but two patients (P13.1 and P20.1) were diagnosed in adulthood. Eleven families (52%) had X-linked family histories. Ten patients (30%) presented with more than one clinical manifestation over time. Ten sibling cases were observed in this study, and seven families manifested different phenotypes. Fifteen patients (45%) were treated with intravenous immunoglobulin replacement therapy. In this study, the mortality rate was 21 of 32 patients (66%), and all the living patients were post-transplanted. Clinical characteristics of this study are summarized in comparison with those of previous study (Table 2).

Hematopoietic stem cell transplantation for patients with XLP-1

Twelve patients with XLP underwent HSCT in Japan (Table 3), and one patient (P9.2) died of *Pseudomonas* sepsis and multiple organ failure 14 days after HSCT. Two patients (P1.2 and P7.2) were transplanted from matched sibling donors, but the other patients were transplanted from matched or one-locus-mismatched unrelated donors, or mismatched familial donors. Various types of conditioning regimen were performed. Five patients (P1.2, P7.2, P9.1, P10.1, and P14.1) underwent HSCT following myeloablative conditioning, but the other patients did so following reduced intensity conditioning (RIC). Acute graft versus host disease (GVHD) was observed in 6 of 11 patients (Grade I, two patients; Grade II, three patients; Grade III, one patient). Chronic GVHD was observed in five patients, among whom 4 (P1.2, P7.2, P10.1, and P18.1) had extensive types and one (P14.1) had a limited type. Eleven patients (92%) have survived and had complete chimerism with a median follow-up of 7 yr and 9 months. A flow cytometric assay could be conducted to evaluate SAP expression in $CD8^+$ T cells and NK cells after HSCT in five patients (P7.2, P10.2, P16.1, P17.2, and P18.1). All the patients demonstrated an increase in SAP expression in $CD8^+$ T cells and NK cells after undergoing HSCT (Fig. 1).

Discussion

X-linked lymphoproliferative syndrome is a rare but life-threatening disease. A large cohort showed that most patients with XLP died by the age of 40 yr and more than 70% of the patients died before the age of 10 yr (2). Early diagnosis in non-familial cases may be difficult because XLP is heterogeneous in its clinical presentation. The ability to screen rapidly and make an accurate diagnosis of patients with XLP facilitates the initiation of life-saving treatment and preparation for HSCT. In a previous study, we generated an anti-SAP mAb, termed KST-3, which was applied to the flow cytometric evaluation of SAP deficiency (XLP-1) (11). All the patients evaluated in this study showed deficient SAP expression, although some patients with missense mutations might demonstrate normal expression of SAP, as shown in Western blotting (16).

Various types of *SH2D1A* mutation have been identified in Japan (11–15). The *SH2D1A*base (http://bioinf.uta.fi/SH2D1Abase) discloses that 133 unrelated patients were identified to have *SH2D1A* mutations. Missense and nonsense mutations appear in one-quarter each, and other types of mutation appear in half of the patients in this database. In the present study, Arg55stop mutations were most frequently found, in keeping with the *SH2D1A*base. No genotype and phenotype correlation was evident in this study, as well as in previous studies (1, 17).

Large cohort studies have shown that the major clinical phenotypes of XLP include FIM (60%), dysgammaglobulinemia (30%), and malignant lymphoma (30%) (1, 2). Aplastic anemia, lymphoid granulomatosis, and systemic vasculitis are minor clinical presentations at frequencies of approximately 3%. Although the present study included a limited number of patients with XLP-1, the distribution of the clinical manifestations seems to be similar to that in previous large studies